INFORMATION TO USERS

The most advanced technology has been used to photograph and reproduce this manuscript from the microfilm master. UMI films the text directly from the original or copy submitted. Thus, some thesis and dissertation copies are in typewriter face, while others may be from any type of computer printer.

The quality of this reproduction is dependent upon the quality of the copy submitted. Broken or indistinct print, colored or poor quality illustrations and photographs, print bleedthrough, substandard margins, and improper alignment can adversely affect reproduction.

In the unlikely event that the author did not send UMI a complete manuscript and there are missing pages, these will be noted. Also, if unauthorized copyright material had to be removed, a note will indicate the deletion.

Oversize materials (e.g., maps, drawings, charts) are reproduced by sectioning the original, beginning at the upper left-hand corner and continuing from left to right in equal sections with small overlaps. Each original is also photographed in one exposure and is included in reduced form at the back of the book.

Photographs included in the original manuscript have been reproduced xerographically in this copy. Higher quality 6" x 9" black and white photographic prints are available for any photographs or illustrations appearing in this copy for an additional charge. Contact UMI directly to order.

U·M·I

University Microfilms International
A Bell & Howell Information Company
300 North Zeeb Road, Ann Arbor, MI 48106-1346 USA
313·761-4700 800 521-0600

Order Number 9111935

Characterization and regulation of platelet activating factor receptors

Gomez, Jorge, Ph.D.

The University of Arizona, 1990

U·M·I
300 N. Zeeb Rd.
Ann Arbor, MI 48106

CHARACTERIZATION AND REGULATION OF PLATELET ACTIVATING FACTOR RECEPTORS.

by

JORGE GOMEZ

A Dissertation Submitted to the Faculty of the
DEPARTMENT OF MICROBIOLOGY AND IMMUNOLOGY
In Partial Fulfillment of the Requirements
For the Degree of

DOCTOR OF PHILOSOPHY
WITH A MAJOR IN MICROBIOLOGY

In the Graduate College
THE UNIVERSITY OF ARIZONA

1 9 9 0

THE UNIVERSITY OF ARIZONA
GRADUATE COLLEGE

As members of the Final Examination Committee, we certify that we have read the dissertation prepared by Jorge Gomez

entitled CHARACTERIZATION AND REGULATION OF PLATELET ACTIVATING FACTOR RECEPTORS.

and recommend that it be accepted as fulfilling the dissertation requirement for the Degree of Doctor of Philosophy.

Marilyn Halonen, PhD	9/24/90 Date
George B. Olson, PhD	Sept. 24, 1990 Date
David W. Sammons, PhD	Sept 24, 90 Date
Henry I. Yamamura, PhD	Sept 24, 90 Date
John D. Palmer, MD, PhD	9/24/90 Date

Final approval and acceptance of this dissertation is contingent upon the candidate's submission of the final copy of the dissertation to the Graduate College.

I hereby certify that I have read this dissertation prepared under my direction and recommend that it be accepted as fulfilling the dissertation requirement.

Dissertation Director Marilyn Halonen, PhD	9/24/90 Date

STATEMENT BY AUTHOR

This dissertation has been submitted in partial fulfillment of requirements for an advanced degree at the University of Arizona and is deposited in the University Library to be made available to borrowers under the rules of the Library.

Brief quotations from this dissertation are allowable without special permission, provided that accurate acknowledgment of source is made. Requests for permission for extended quotation from or reproduction of this manuscript in whole or in part may be granted by the copyright holder.

SIGNED: Jorge Gomez

ACKNOWLEDGMENTS

I greatefully acknowledge Dr. Marilyn Halonen, my Dissertation Director for her patience, support, and contribution to this work. Special thanks are extended to Drs. Henry I. Yamamura and John W. Bloom, for their ideas and their generous support to this work. I also thank my committee members, Drs. George Olson, David Sammons, and John Palmer for their valuable advice. Particular thanks are extended to Carla Lohman, Joyce Trombley, and David Wu for their technical support and assistance. I thank my lovely wife Susana, my parents, and brothers for their encouragement and support to the realization of this work.

TABLE OF CONTENTS

LIST OF ILLUSTRATIONS

LIST OF TABLES

ABSTRACT

Platelet activating factor (PAF) is a potent mediator in a variety of inflammatory events. Determining whether PAF participates in the bronchial hyperresponsiveness characteristic of asthma is the long term objective for which the studies described here represent an initial step. PAF is a potent agonist that causes contraction of guinea pig peripheral lung strips. To determine if specific receptor sites for PAF could be demonstrated in guinea pig lung membranes (GPLM), direct radioligand binding studies were performed with [^{3}H]C_{16}-PAF (1-*O*-hexadecyl-2-acetyl-*sn*-glycero-3-phosphocholine) and the PAF antagonists [^{3}H]WEB 2086 and [^{3}H]RP52770. Binding parameters were compared to those from rabbit platelet membranes (RPM). These studies demonstrated specific binding sites for [^{3}H]C_{16}-PAF of high affinity in GPLM with a K_d of 3 nM; and in RPM with a K_d of 1 nM. [^{3}H]C_{16}-PAF identified receptor densities in GPLM of 200 fmol/mg protein and in RPM of 1922 fmol/mg protein. In both tissue preparations binding of [^{3}H]C_{16}-PAF was inhibited to the same maximum degree by C_{16}-PAF, C_{18}-PAF, WEB 2086, and RP52770, all with pseudo-Hill coefficients of unity. The PAF antagonist [^{3}H]WEB 2086 identified a receptor density similar to that of [^{3}H]C_{16}-PAF. The binding of [^{3}H]WEB 2086 was inhibited to the same degree by C_{16}-PAF, C_{18}-PAF, WEB 2086 and RP52770, indicating WEB 2086

and PAF interact at the same receptor sites in both GPLM and RPM. Although inhibition curves for antagonists yielded pseudo-Hill coefficients of unity, inhibition by agonists yielded shallow inhibition curves suggesting two types or states for the PAF receptor. The PAF antagonist [^{3}H]RP52770 was found to be an unsuitable ligand because it labeled a much larger density of binding sites (1200 fmol/mg protein in GPLM, and 10105 fmol/mg protein in RPM) and was inhibited to little or no extent by C_{16}-PAF, C_{18}-PAF, WEB 2086 or lyso-C_{16}-PAF. Studies of signal transduction suggest that the binding affinity of the agonists C_{16}-PAF and C_{18}-PAF (but not for the antagonist WEB 2086) is regulated by GTP-gamma-S and Na^+, providing indirect evidence that the PAF receptor in both tissue preparations is coupled to a guanine nucleotide regulatory protein. However, agonist binding retained shallow inhibition curves indicating heterogeneity of sites with respect to this regulation. Binding affinity for the agonists was not affected by cholera toxin or pertussis toxin. These results indicate PAF receptors in lung tissue could not be distinguished from those in RPM, however, both tissues appear to show heterogeneity of binding indicating the existence of receptor subtypes or states.

CHAPTER I

INTRODUCTION

Historical Background

Platelet activating factor (PAF) is a potent autocoid released in a variety of inflammatory events. Several lines of evidence indicate that PAF might be involved in bronchoconstriction and the induction of bronchial hyperresponsiveness thereby contributing to asthma (4). Early experiments showed that leukocytes from antigen-sensitized rabbits released a soluble factor or factors capable of inducing the release of mediators from rabbit platelets (3,31,75,77). At that time, nothing was known about the molecular structure of this mediator and the name of platelet activating factor was derived. Subsequent experiments demonstrated that this activation of rabbit platelets was a result of an IgE-dependent activation of basophils (7). Subsequent studies suggested a lipid-like molecule (6), and its chemical structure was later described as a mixture of 1-*O*-hexadecyl-/ and 1-*O*-octadecyl-2-acetyl-*sn*-glycero-3-phosphocholine (22,27). These molecules are referred herein as C_{16}-PAF and C_{18}-PAF, respectively. Multiple molecular species of PAF were later shown to be released from stimulated polymorphonuclear leukocytes and were structurally characterized (63). These included several 1-O-alkyl homologues, 1-O-acyl analogues, and

acetylated phosphoglycerides with polar head groups other than choline (53,60,63,68). However, most of the studies aimed at elucidating the pathobiological activity of PAF have been focused on the prototype molecules: C_{16}-PAF and C_{18}-PAF, shown in Figure 1. At present, there is very little information regarding the activities of the other spectrum of the PAF molecules. Preliminary studies based upon structure relationships of the different PAF molecules suggest that minor structural alterations have major effects on biological activities (22,26,35). For instance, the concentration of C_{16}-PAF to cause 10% (ED_{10}) secretion of lysosomal enzymes from human PMN was 8.9 nM, whereas the ED_{10} for C_{18}-PAF was 340 nM, a difference of about 40-fold. Similarly, substitutions of the polar head (choline) have resulted in decreased potency or biological activity (64) and removal of the acetyl group resulted in complete loss of activity. Furthermore, there are no studies addressing synergistic or antagonistic actions of the different PAF molecules. Thus, individual PAF molecular species of PAF must be rigorously characterized in terms of their biological activity, and synergistic or antagonistic mechanisms with other PAF molecules in order to understand the role(s) of the whole spectrum of the PAF family of molecules.

Figure 1. Representative species of platelet activating factor.

A. 1-*O*-hexadecyl-2-acetyl-*sn*-glyceryl-3-phosphorylcholine (C_{16}-PAF):

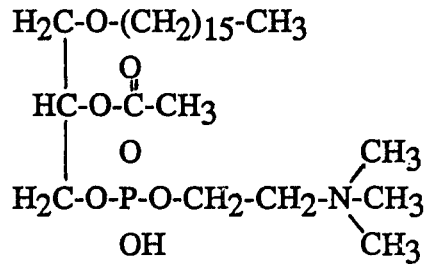

B. 1-*O*-octadecyl-2-acetyl-*sn*-glyceryl-3-phosphorylcholine (C_{18}-PAF):

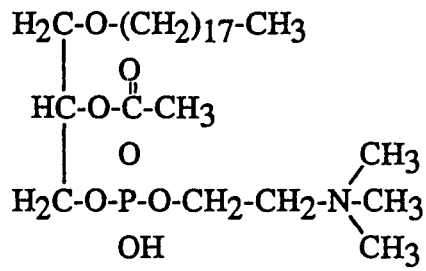

C. 1-*O*-hexadecyl-*sn*-glyceryl-3-phosphorylcholine (lyso-C_{16}-PAF):

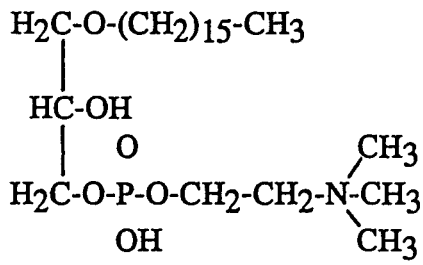

Biological Activities of PAF

PAF is not stored as a preformed molecule; rather it is rapidly generated upon cell stimulation. Cells involved in biosynthesis and release include cells that participate in broad spectrum of inflammatory reactions: platelets (17), PMNs (45), monocytes (12), eosinophils (45), and macrophages (30), including alveolar macrophages (47). The nature of the cells involved in PAF biosynthesis and release explains in part why this autacoid might be important in regulating acute and chronic inflammatory processes.

Several <u>in vitro</u> studies have shown that PAF induces a variety of activities in cells involved in inflammatory events including: aggregation and secretion of platelets, PMNs, monocytes (51,59) and eosinophils (10); activation of peritoneal and alveolar macrophages (2,28), and endothelial cells (9,11); and contraction of smooth muscle (79,80), among others. In human and rabbit PMN, PAF induces aggregation, chemotaxis, and lysosomal enzyme secretion including ß-glucuronidase secretion in a dose-dependent manner (59,76). In addition, PAF causes the initiation of the respiratory burst in human PMN as depicted by the production of superoxide anion (51). Similarly, in guinea pig peritoneal macrophages, PAF activates the respiratory burst and induces the synthesis of PGE and TxB_2 (28). In guinea pig alveolar macrophages, PAF induces mobilization of

arachidonic acid in a dose-dependent manner (2). In addition, PAF is a potent chemotactic factor for eosinophils and induces degranulation and LTC_4 production (10). PAF causes a sustained contraction of isolated human (79) and guinea pig peripheral lung strips (80). In both tissues, the PAF-induced contraction is dose-dependent and is not blocked by H_1-blockers, or inhibitors of prostaglandin or leukotriene synthesis. The action of PAF in guinea pig lung strips appear to be platelet independent.

Several <u>in vivo</u> studies have shown that i.v. infusion of PAF induces hemoconcentration, vascular pemeability and systemic hypotension (49). The increased vascular permeability may be due to a direct effect of PAF on endothelial cells. Following infusion or transtracheal administration of PAF in the rabbit, a marked accumulation of platelet and leukocytes is observed in the pulmonary circulation (50). Subsequently, leukocytes (mostly PMNs and eosinophils) infiltrate the lung parenchyma and persist for more than 96 hrs thereafter. In some species, PAF has been shown to mediate bronchoconstriction. In guinea pigs, aerosolized administration of PAF causes bronchoconstriction and induces bronchial hyperresponsiveness (18). The PAF-evoked bronchoconstriction is leukotriene- and platelet-independent and antagonized by PAF antagonists.

In humans, aerosolized administration of PAF to normal subjects causes a dose-dependent bronchoconstriction and also an increase in non-specific bronchial hyperresponsivenss to methacholine (19). Subsequent studies demonstrated further the PAF-evoked bronchoconstriction was specific to PAF since it was markedly decreased by PAF antagonists (71). These studies further support the hypothesis that PAF is involved in a variety of acute and chronic inflammatory processes, including asthma (86).

Role of PAF in Asthma and Systemic Anaphylaxis

Allergic asthma is characterized by an abnormal responsiveness of the airways to allergens, accompanied by abnormal generation and clearance of airway secretions (55). In general, allergic asthma is a manifestation of type I hypersensitivity reactions, which is characterized by high levels of IgE antibodies in susceptible populations of individuals. Generally speaking, a few exposures of these individuals to allergens gives rise to the synthesis of high levels of IgE antibodies, which bind to mast cells and basophils. Subsequent antigen challenge causes release of mediators. Most of these mediators have vasoactive and inflammatory properties and are smooth muscle activators. Histamine, leukotrienes, PAF, and prostaglandins are some of the most important mediators released by this mechanism.

Hence, this mechanism of allergen-IgE-mast cell or allergen-IgE-basophil secretion of mediators is responsible for triggering episodes of allergic rhinitis, allergic asthma, and anaphylactic reactions. Therapy has been directed primarily at inhibiting the release of mediators and inducing bronchodilation (69). However, late-phase reactions which appear 24 to 48 hrs following antigen challenge have been characterized by bronchial hyperresponsiveness and cellular infiltrates. Cell infiltrates are composed mainly of neutrophils, eosinophils, and monocytes, which contribute to the inflammatory component of the disease. Bronchial hyperresponsiveness is the most important feature of bronchial asthma and is characterized by an enhanced contractile response of airways to diverse stimuli, which include allergens; pharmacologic agents such histamine, cholinomimetics and leukotrienes; and physical stimuli such as cold air and dust. Bronchoalveolar eosinophilia is characteristic of bronchial infiltrates and is more pronounced in subject undergoing late-phase reactions (20).

PAF has been shown to be an important inflammatory mediator in the lung. PAF induces <u>in vivo</u> pathologic changes that mimic many features of asthma, including enhanced vascular permeability, chemotaxis of neutrophils, platelets, and especially eosinophils, and stimulation of

mucus secretion (4). Evidence has shown that PAF induces bronchoconstriction *in vivo* and contracts human lung strips *in vitro* (80). However, it is not clear whether PAF exerts these effects through direct or indirect mechanisms. It has been suggested that the role of PAF is to induce the late-phase inflammatory process (61). In this proposed mechanism, PAF is released in the lungs and acts as a chemotactic factor for eosinophils. Eosinophils migrate to the lung and release a number of mediators that leads to damage of the airway epithelium. This leads to denudation of the airway epithelium, enhancing access to airway smooth muscle. This denudation of the airways and enhanced access to airway smooth muscle may result in increased sensitivity to a variety of spasmogens resulting in airway hyperresponsiveness. In addition, denudation of epithelial cells in the airways may impair mucous production and secretion, and thus may decrease removal of unwanted materials from the lung via the mucociliary escalator. Intratracheal challenge with PAF causes cellular infiltration in the bronchi, damage to the airway epithelium, impairment of mucus production, and bronchial hyperresponsiveness (19). Recent studies assessed the presence of the PAF in bronchoalveolar lavage from 28 asthmatic subjects (78). Eight of these asthmatic subjects had measurable amounts of PAF (0.5 to 7.1 nM) in the

supernatant, and was significantly associated with high levels of lymphocytes, low levels of neutrophils, and high macrophage metabolic activity. Contrary, normal subjects had no detectable levels of PAF in supernatants. Thus, the pathologic and inflammatory changes observed in clinical asthma are closely mimicked by exposure to PAF, and PAF has been detected in the lung fluid of at least some asthmatics, suggesting that PAF might be one of the major mediators in clinical asthma.

Specific Receptors for PAF

Early observations based on the biological activities of PAF strongly suggested that the actions of PAF were receptor-mediated. Specific receptors for PAF have been partially characterized using radioligand binding studies. Initial characterization of specific binding sites utilized tritium-labeled and unlabeled PAF as ligands. Previous studies have characterize [^{3}H]PAF interaction with its binding site as reversible, saturable, and of relative high affinity. However, reports on the binding affinity and receptor densities of [^{3}H]PAF showed discrepancies between different investigators. In human platelets, the binding of [^{3}H]PAF showed a binding affinity that ranges from 0.016 to 37 nM, a 1000 fold range difference (82,83). Receptor densities ranged from 240 to 1400 sites/cell. In human PMN,

some investigators have reported data suggesting a second binding site (58), however other investigators have reported a single binding site for [^{3}H]PAF in this cell type (48). These reported differences, regarding the number of receptor sites/cell and binding affinities might be accounted for in most cases by the use of radiolabeled agonist for binding, [^{3}H]PAF. Different experimental conditions may also contribute to those differences observed in the binding parameters. These conditions include type of buffer used, incubation temperature, method of separating radioligand bound/free, among others. The recent availability of PAF receptor antagonists have helped to characterize PAF binding sites. Specifically, the PAF antagonist RP52770, shown in Figure 2A (a pyrrolothiazole derivative) was reported to antagonize the <u>in vitro</u> PAF-evoked platelet aggregation in rabbit platelets (70). In addition, [^{3}H]RP52770 binding displayed high affinity for the PAF receptor on rabbit platelet membranes and human PMN (48,70). However, [^{3}H]RP52770 was shown to identify additional binding sites in human platelets, besides the PAF binding site (82). A second PAF antagonist termed WEB 2086 shown in Figure 2B (a triazolobenzodiazepine derivative) has been shown to antagonize the <u>in vivo</u> and <u>in vitro</u> effects of PAF (14). The binding properties of [^{3}H]WEB 2086 were evaluated in intact human platelets. A single binding site of relative

Figure 2A. PAF antagonist RP52770.

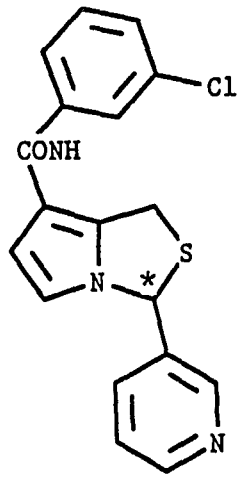

Figure 2B. PAF antagonist WEB2086.

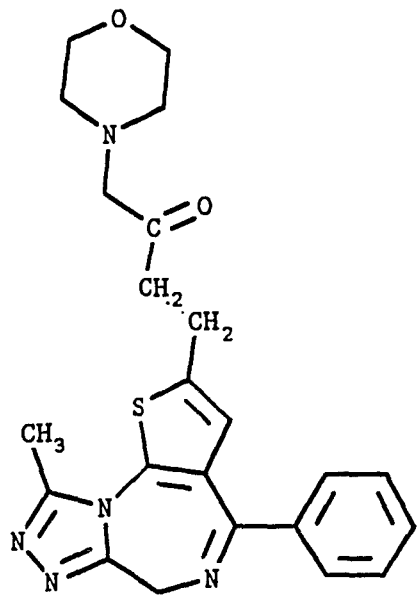

high affinity has been described (82). These studies also showed that WEB 2086 inhibited [^{3}H]PAF binding in a dose dependent manner and that [^{3}H]WEB 2086 bound approximately the same number of sites as [^{3}H]PAF. A third PAF antagonist, termed L-659,989, has been shown to antagonize PAF-induced aggregation of rabbit platelets *in vitro*, and PAF-induced extravasation in rats *in vivo* (66). In addition, [^{3}H]L-659,989 was shown to identify the same sites as [^{3}H]PAF in rabbit platelet membranes (36). The binding of [^{3}H]L-659,989 is inhibited in a dose dependent manner by unlabeled C_{16}-PAF and C_{18}-PAF.

In addition to radioligand binding studies to characterize PAF receptors, several other types of studies have suggested the existence of PAF receptors in different cells and tissues. In rabbit neutrophils (54) and human monocytes (56) PAF induced phosphoinositide biosynthesis in a dose-dependent manner. In human and rabbit platelet membranes, PAF induces GTPase activity which was abolished by PAF antagonists (34,37). Altogether, these observations strongly suggest the existence of PAF receptors, on platelets and PMN's as evidenced by radioligand binding studies with tritium-labeled PAF and various antagonists. The data suggests that PAF receptors on these cells are coupled to guanine nucleotide regulatory proteins.

CHAPTER II

MATERIALS AND METHODS

Preparation of Guinea Pig Lung Membranes (GPLM)

Hartley guinea pigs of either sex weighing 300 to 400 g were sacrificed by decapitation and peripheral lung tissues were rapidly excised and placed in 9 volumes of cold 50 mM Tris buffer, pH 7.4. All of the following procedures were carried out at 4°C. Suspended tissue was homogenized at setting 10 on a Polytron (Brinkman Instruments, Inc., Westbury, NY) with three 30 sec bursts separated by 30 sec pauses. The homogenate was centrifuged at 1200 x *g* for 5 min and the pellet discarded. The supernatant was centrifuged at 40000 x *g* for 15 min. The resulting pellet was resuspended in 50 mM Tris, 5 mM $MgCl_2$, pH 7.4, which was used for the binding assay. Protein concentrations were determined by the bicinchoninic acid method (Pierce, Rockford, IL) using bovine serum albumin (BSA) as standard.

Preparation of Rabbit Platelet Membranes (RPM)

Rabbit platelet membranes were prepared by collecting blood from the marginal ear artery of New Zealand White rabbits in sodium citrate (0.38%, w/v final). Blood samples were immediately centrifuged at 150 x *g* for 30 min at room temperature. The platelet rich plasma layer (top) was carefully removed, diluted with an equal volume of normal

saline solution and mixed gently but thoroughly. Diluted platelet rich plasma was layered onto 2 ml of Ficoll-Paque (Pharmacia, Piscataway, NJ) and centrifuged at 1000 x *g* for 20 min. The top plasma layer was discarded and the layer of platelets at the top of the Ficoll-Paque was transferred into large centrifuge tubes. The collected platelets were suspended in 5 volumes of normal saline solution and centrifuged at 1500 x *g* for 20 min. Pellets were resuspended in normal saline, and the cell number adjusted to 1-2 x 10^8 platelets/ml, centrifuged at 1500 x *g* for 20 min and the supernatant discarded. Routinely, the cell recovery was 60-70% of the starting cell concentration. Pelleted platelets were stored at -70°C until used. Frozen platelets were thawed and suspended in cold 50 mM Tris, 5 mM $MgCl_2$, and pH 7.4. Suspended cells were homogenized with three 30 sec bursts separated by 30 sec pauses with a tissue homogenizer. Homogenates from platelet membranes were centrifuged at 40000 x *g* for 15 min and the resulting pellet was resuspended in buffer for the binding assay.

Pharmacological Agents

The PAF species 1-*O*-hexadecyl-2-*sn*-glyceryl-3-phosphorylcholine (C_{16}-PAF), 1-*O*-octadecyl-2-*sn*-glyceryl-3-phosphorylcholine (C_{18}-PAF), and 1-*O*-hexadecyl-*sn*-glyceryl-3-phosphorylcholine (lyso-PAF) were obtained from Bachem,

Corp. (Torrance, CA). The following tritium labeled compounds were obtained from New England Nuclear (Boston, MA): C_{16}-PAF (alkyl-labeled, 56.7 Ci/mmol; acetyl-labeled, 10 Ci/mmol), 3-(4-(2-chlorphenyl)-9-methyl-6H-thieno(3,2-f)-(1,2,4)triazolo(4,3-a)(1,4)diazepine-2-yl)-1-(4-morpholinyl)-1-propane (WEB 2086, 14.1 Ci/mmol), N-(3-chlorophenyl)-3-(3-pyridinyl)-1H,3H-pyrrolo[1,2-c]thiazole-7-carboxamide (RP52770, 24.1 Ci/mmol). Unlabeled WEB 2086 was a gift from Boehringer Ingelheim. Unlabeled RP52770 was kindly provided by Dr. I. Cavero (Rhône-Poulenc, Sante, France). BSA, pertussis and cholera toxins, adenosine 5′-triphosphate (ATP), guanosine 5′-triphosphate (GTP), guanosine 5′-0-3-thiotriphosphate (GTP-gamma-S), phorbol 12-myristate 13-acetate (PMA), and pepsin were obtained from Sigma Chemical Co. (St. Louis, MO).

Radioligand Binding Assays

Basic Conditions: In order to estimate the different binding parameters, radioligand binding reactions were carried out by mixing homogenized tissue with radioligands, followed by incubation and then filtration to remove free ligand. These radioligand binding experiments were carried out in 50 mM Tris buffer containing 5 mM $MgCl_2$ and 2.5 mg/ml of BSA at pH 7.4.

Definition of Specific Binding: Preliminary experiments were carried out using [^{3}H]C_{16}-PAF as ligand. Specific binding was defined as the difference between total and nonspecific binding. Total binding was the observed binding in the absence of any inhibitor. Nonspecific binding was defined as that binding in the presence of 10 μM C_{16}-PAF, 100 μM WEB 2086, or binding to the glass fiber filters.

Subsequent experiments were carried out using [^{3}H]WEB 2086 and [^{3}H]RP52770 as ligands. For [^{3}H]WEB 2086, specific binding was determined as the difference between radioligand bound in the absence and presence of 10 μM C_{16}-PAF or 100 μM WEB 2086. Specific binding for [^{3}H]RP52770 was determined as the difference between radioligand bound in the absence and presence of 100 μM RP52770.

Determination of the Tissue Concentration: For all the studies the assay volume was 1 ml with a final protein concentration of 0.3 to 0.7 mg/ml for GPLM, and 0.02 to 0.05 mg/ml for RPM. These concentrations are in the range of linearity of [^{3}H]C_{16}-PAF binding (Figure 3). For all radioligands, tissue concentration was limited so that the concentration of the free radioligand did not change appreciably during the binding assay.

Termination of Binding Reactions: Binding reactions were terminated by filtering the incubation mixture through

fiber glass filters (Whatman, GF/B). A Brandel cell harvester apparatus (Gaithersburg, MD) was used for [^{3}H]C_{16}-PAF and [^{3}H]RP52770. For [^{3}H]WEB 2086 a single filter holder apparatus was used (model FH 224; Hoefer Scientific Instruments, San Francisco, CA). Filters were presoaked in cold incubation buffer for at least 1 hr to decrease nonspecific binding to the filters. After filtration, each filter was rinsed three times with 4 ml of ice-cold incubation buffer. The rinsing volume was determined experimentally by allowing the binding reaction to occur, then washing the filters with different volumes of incubation buffer (Figure 4). Receptor bound radioactivity retained in the filters was extracted for 4 hrs with 6 ml of liquid scintillation cocktail. The scintillation cocktail was prepared by mixing two liters of toluene (Baker, Phillispsburg, NJ), 1 liter of Triton X-100 (Westchem, San Diego, CA) and 16 gm of Crystal-fluor (Westchem). Radioactivity was determined by liquid scintillation spectrophotometry (Beckman Instruments, Fullerton, CA) at a counting efficiency of 60%.

Figure 3A.

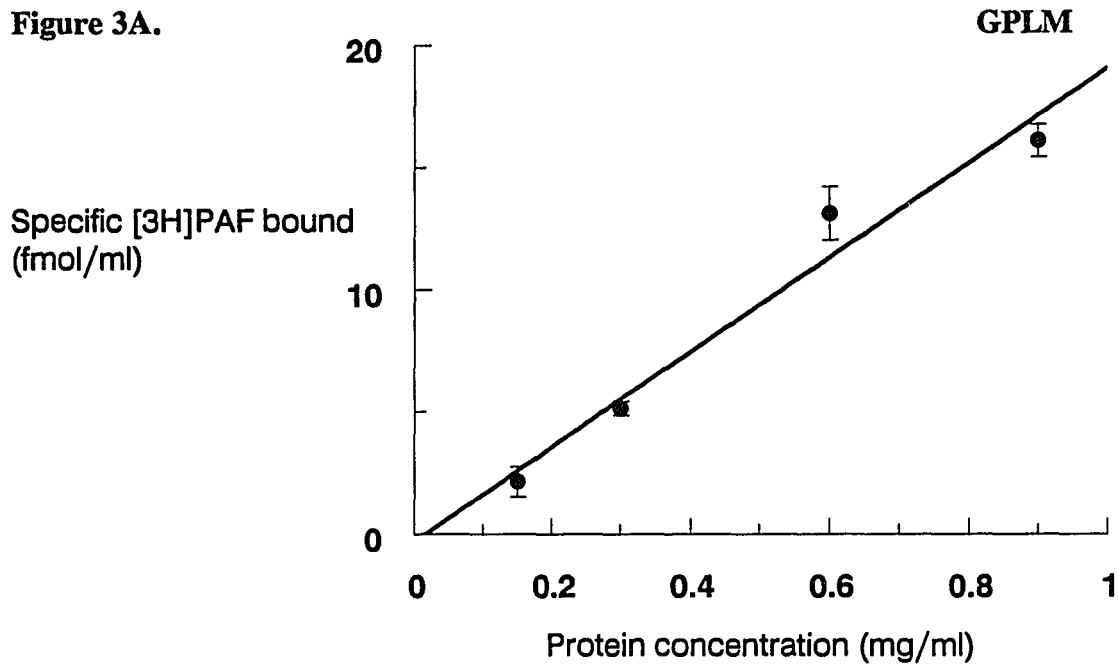

Figure 3B.

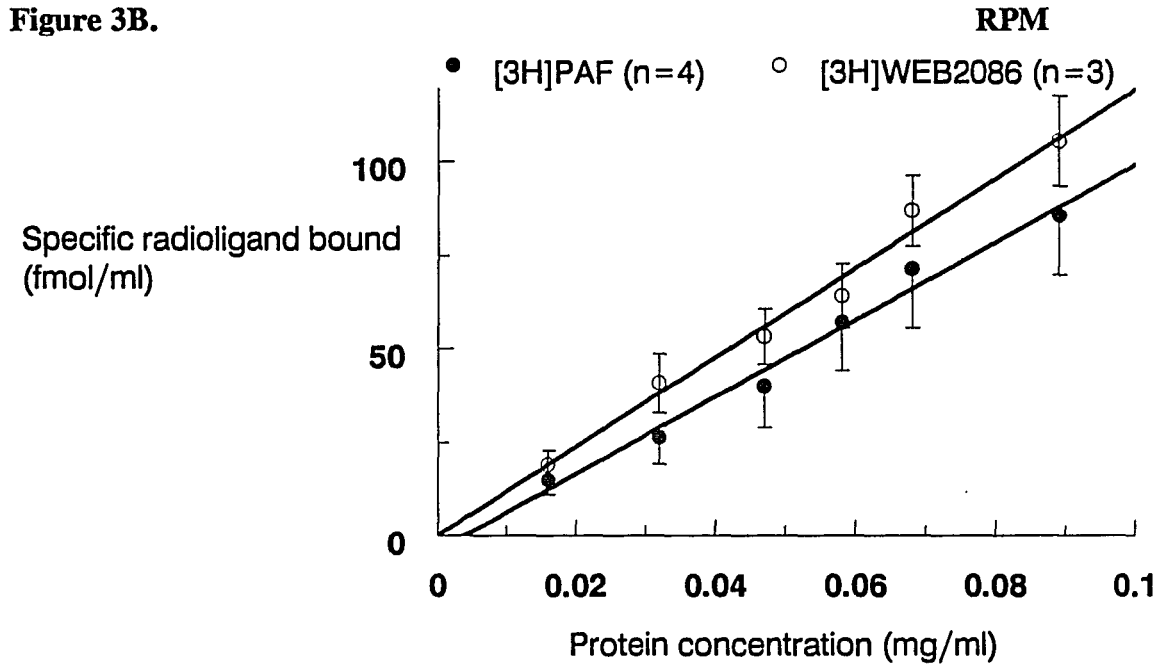

Figure 3. Specific binding of 1 nM [^{3}H]C_{16}-PAF to GPLM (3A) was linear between 0.15 to 0.9 mg protein/ml ($n=3$). Specific binding of 1 nM [^{3}H]C_{16}-PAF and 5 nM [^{3}H]WEB2086 to RPM (3B) was linear between 0.015 to 0.09 mg protein/ml. Data points represent the mean ± SEM.

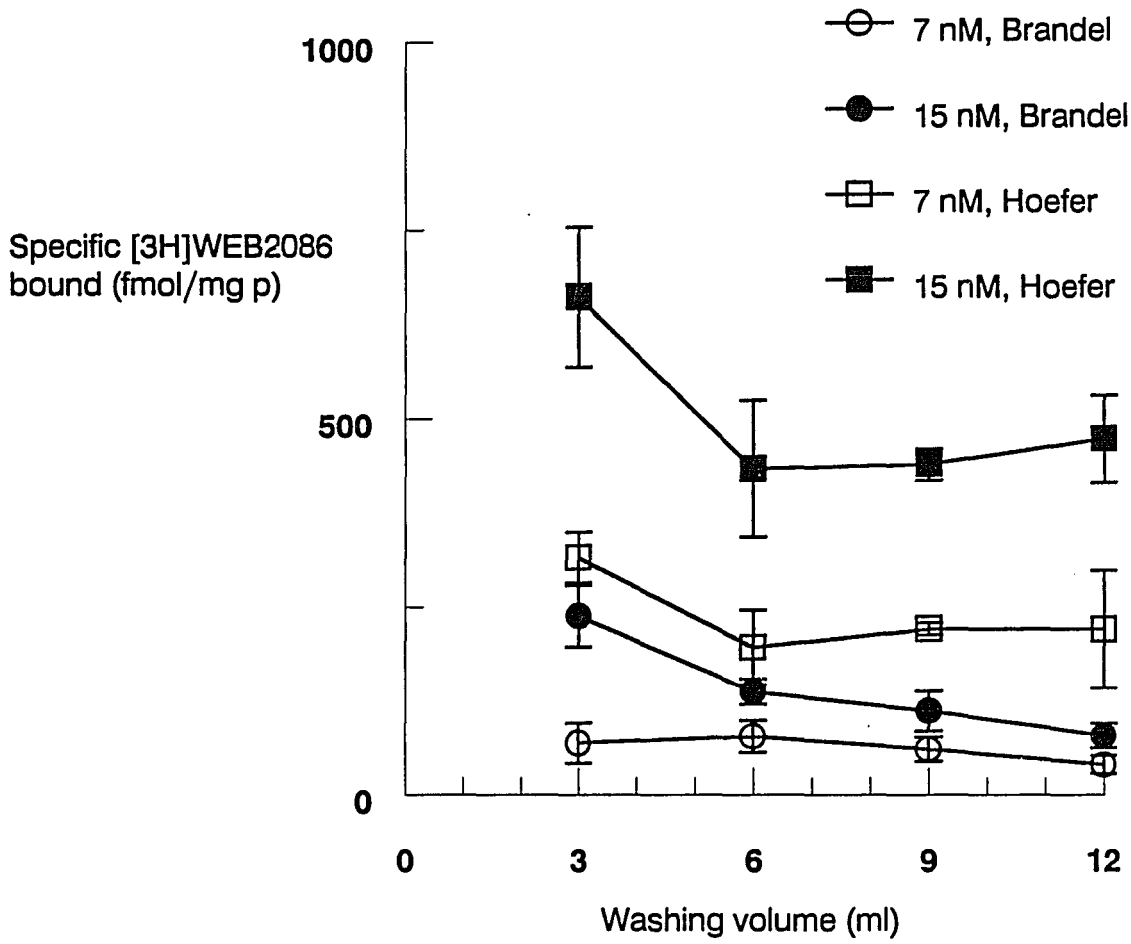

Figure 4. Effects of washing volumes on specific binding of 7 and 15 nM [^{3}H]WEB2086 to GPLM. Membranes were incubated for 4 hrs at 4°C and filtered through fiber glass filters using either a Brandel or Hoefer apparatus. Subsequent binding experiments using [^{3}H]WEB2086 as ligand were terminated using a Hoefer apparatus with 9 mls of washing solution. Data point represent the mean ±SEM of 3 separate experiments.

Other Conditions: All measurements were done in duplicate in at least four separate experiments. Throughout the experimental procedures, the temperature was kept at 4°C unless otherwise indicated. The incubation time for all radioligands was determined experimentally by kinetic studies. The BSA was needed to provide PAF solubility in aqueous media. Initial experiments were carried out to determine the optimal BSA concentration. As shown in Figure 5, BSA inhibited both specific and nonspecific binding of [^{3}H]C_{16}-PAF (0.5 nM) to GPLM, but at concentrations of 2.5 mg/ml or less, the effect was primarily to reduce nonspecific binding. Specific binding accounted for 50% of the total [^{3}H]C_{16}-PAF binding at a BSA concentration of 2.5 mg/ml, which was selected as the concentration for subsequent experiments.

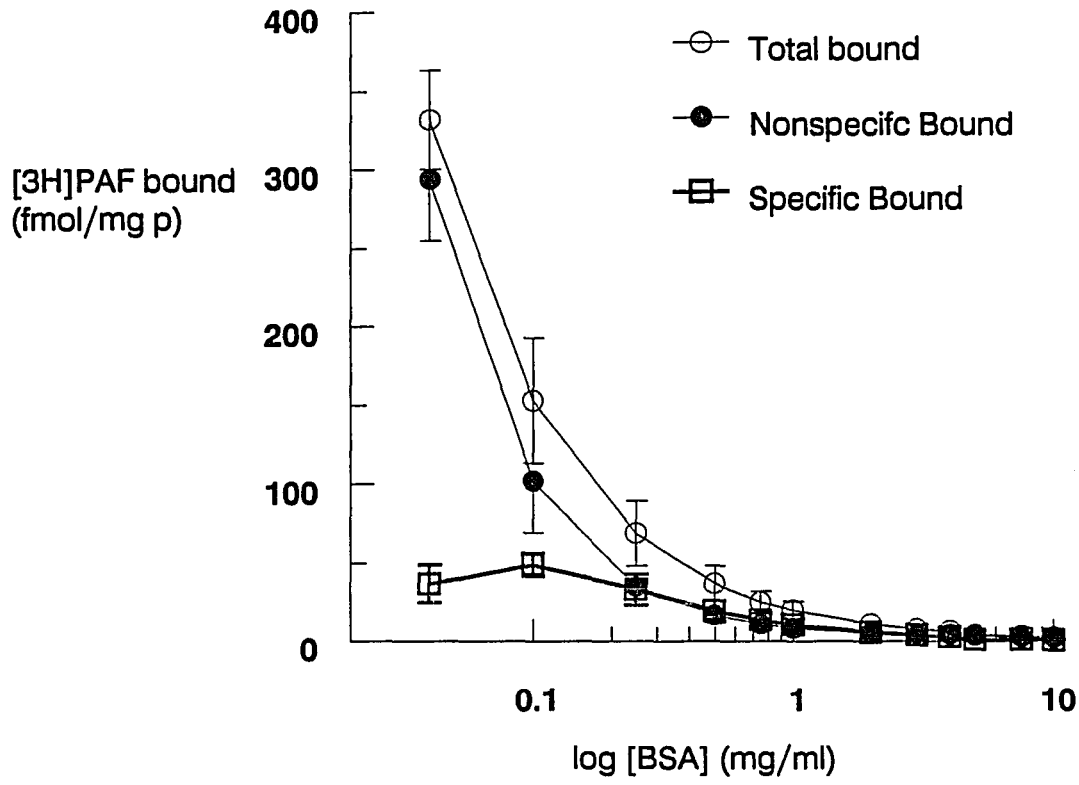

Figure 5. Effects of BSA on binding of 0.5 nM [^{3}H]PAF to GPLM. Membranes were incubated with 0.5 nM [^{3}H]C_{16}-PAF and at increasing concentrations of BSA (0.05 to 10 mg/ml), in the presence (nonspecific bound)or absence (total bound)of 10 μM WEB2086. Specific binding was estimated as the difference between total and nonspecific radioligand bound. Data points represent the mean $\pm$ SEM of 4 separate experiments.

Kinetic Experiments

Association Experiments: The purpose of these experiments was to determine the ligand association rate constant (k_{+1}) and to establish the time when the ligand-receptor complex had reached a steady state condition. Since this reaction depends on the concentration of the radioligand and receptor, experiments were done at radioligand concentrations below the estimated K_d from saturation studies (see below). For the calculation of k_{+1}, a second order equation was used (87), where the observed association rate (K_{obs}) of radioligand binding is dependent on the initial concentration of the radioligand ([L]) bound at equilibrium (Be) and the concentration of receptor sites (RT). This is described by the following equation: $RT=[Be](1-e^{Kobs.t})$. The k_{+1} is estimated as follows: $k_{+1}=K_{obs}-k_{-1}/[L]$. The k_{-1} is the dissociation rate constant determined in separate experiments (see below) and [L] is the concentration of the radioligand used.

Dissociation Experiments: To determine reversibility of the ligand-receptor complex and to estimate the dissociation rate constant (k_{-1}), radioligand and receptor were allowed to reach a steady state and then an excess amount of unlabeled drug (100 μM WEB 2086) was added in order to induce dissociation of the radioligand. This experiment provides a measurement of the dissociation

reaction which follows first order process since it depends only on the initial concentration of the complex (87). The first order rate reaction is described as follows: $[Rbt]=[Rb0].e^{-k_{-1}.t}$, where [Rbt] is the amount of radioligand bound at time t, Rb0 is the amount of radioligand bound at t=0.

Saturation Experiments

In order to determine the equilibrium dissociation constant (K_d) and the maximum number of binding sites, saturation experiments were done by incubating increasing concentrations of the radioligand with a fixed concentration of tissue. Nonspecific binding was determined as described above, according to the radioligand used. The K_d and Bmax are derived from nonlinear regression analysis using the equation that describes the relationship between the radioligand bound (B) to the receptor and free concentration of radioligand (L) is: $B=(Bmax)(L)/(K_d+L)$. This equation describes a rectangular hyperbolic relationship between the radioligand bound to the receptor and the free ligand concentration. Linearized transformations were also used to analyze these data by plotting B/L as a function of B. This equation was originally described by Scatchard (74) and adapted by Rosenthal (73) for receptor binding studies, where $B=Bmax-K_d(B/L)$. The K_d is negatively reciprocal to

the slope of the line, and the Bmax is the intercept on the abscissa.

Inhibition Experiments

In order to establish the pharmacological profile of the PAF receptors, membranes were incubated with a fixed concentration of radioligand and with varying concentrations of unlabeled ligand or inhibitor (D). As the concentration of the unlabeled ligand increases, it will compete with the radioligand for the receptor binding site decreasing the radioligand-bound receptor complex. This will be expressed as a percentage of the control (amount of radioligand bound in the absence of the unlabeled ligand). Inhibition data are plotted as radioligand bound (%B of control) on the ordinate against the log of the concentration of unlabeled ligand on the abscissa. A sigmoidal curve is used to fit inhibition data with the following equation: $B=(Bmax)/(1+(D*IC_{50}))$, where IC_{50} is the concentration of the unlabeled ligand that inhibits 50% of the specific binding (B) as described by Rodbard (72). In order to study the possibility of receptor subtypes and/or positive cooperativity between ligand-receptor interactions, inhibition data were also transformed to a linearized form using the equation described by Hill (32), where the log(B/100-B) is plotted against log [D] and the slope of the

linear regression line is the pseudo-Hill coefficient (n_H). Thus, when n_H=1.0 it is interpreted as a bimolecular interaction: one ligand molecule interacting with a one class of binding sites. However, if n_H<1.0 it is interpreted as a negative interaction, more than one binding site or receptor subtypes. Alternatively, if n_H>1.0 it is interpreted as positive cooperativity (the binding of one molecule facilitating the binding of the next molecule).

Metabolism of Radioligand

Binding of [^{3}H]C_{16}-PAF (acetyl labeled): In order to establish if [^{3}H]C_{16}-PAF is degraded during the incubation period of binding studies by metabolic enzymes present in the tissue, saturation studies were done using [^{3}H]C_{16}-PAF (acetyl-labeled, 10 Ci/mmol) and compared with saturation studies with [^{3}H]C_{16}-PAF (alkyl labeled, 56.7 Ci/mmol) using filtration techniques previously described. In addition, in separate experiments tissue was incubated with increasing concentrations of [^{3}H]C_{16}-PAF (acetyl labeled) as outlined in Figure 6. The binding reaction was terminated by centrifuging the tubes at 40000 x *g* for 10 min. The supernatant was recovered (about 0.95 ml) and precipitated with 0.25 ml of (50% v/v) trichloro acetic acid (TCA) for 10 min. The precipitated mixture was then centrifuged at 40000 x *g* for 10 min and the amount of radioactivity determined in

both pellet and supernatant. With the acetyl-labeled ligand the presence of cellular or serum acetylhydrolase will decrease the specific binding on filtration experiments, and substantial radioactivity will be recovered in the supernatant after TCA precipitation followed by centrifugation.

Rebinding Experiments: In order to test for the presence of anomalous inhibitors present on the tissues and/or ligand degradation, tissue was incubated with known concentrations of radioligand, followed by centrifugation at 40000 x *g* for 10 min, recovery of the supernatant and incubation (rebinding) with fresh tissue under equilibrium conditions. Specific binding determined from these experiments was compared to a control obtained from using fresh tissue and concentrations of fresh radioligand equivalent to that in the supernatant of the paired experiment, as outlined in Figure 7. A decrease in specific binding in the rebinding experiment when compared to control was interpreted as radioligand degradation or the presence of endogenous inhibitors of binding in the tissue.

Figure 6. Binding of [^{3}H]C_{16}-PAF (acetyl-labeled) to GPLM

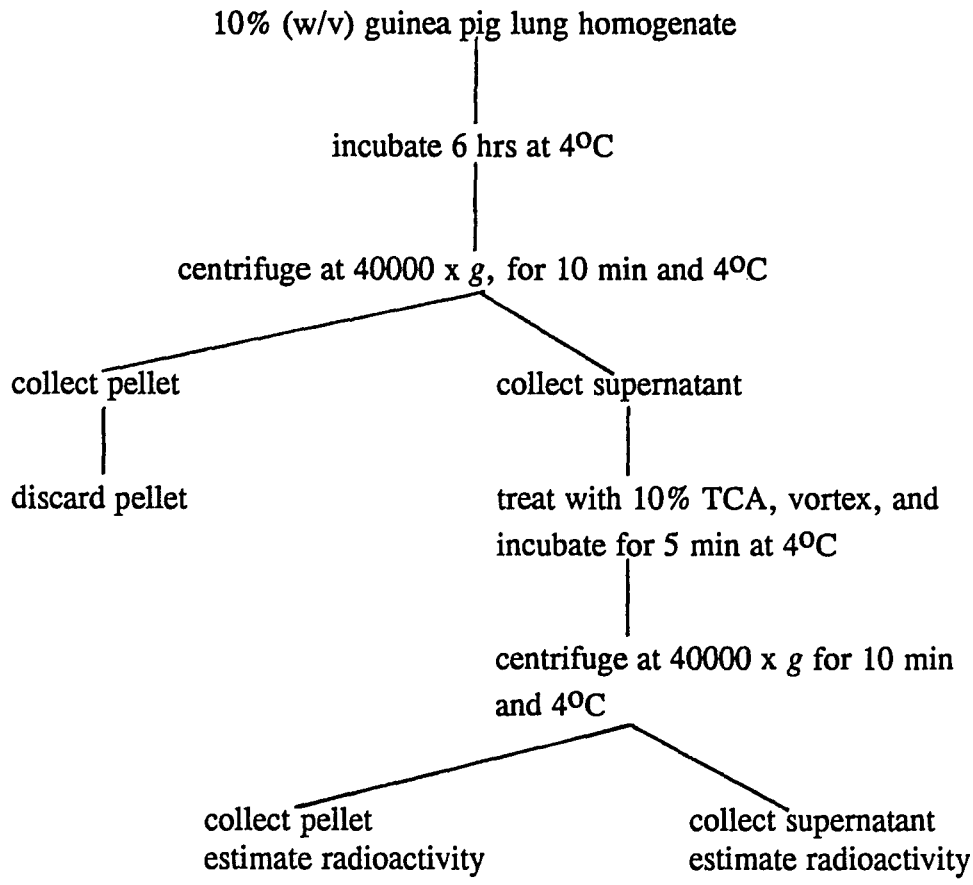

Receptor Digestion

In order to test for suceptibility of the receptor to heating, homogenized membranes were incubated in a boiling water bath for 15 min followed by immersion in a ice-cold water bath for an additional 15 min. The resulting membranes were then used for binding studies as previously described. In order to test for proteolytic suceptibility, homogenized membranes were incubated with pepsin for 4 hrs and at 25°C. Suspended membranes were centrifuged for 15 min at 40000 x *g* and 4°C. The resulting pellet was resuspended in buffer and used for binding studies as described above.

Regulation of Binding

In order to test for the effects of putative guanine nucleotide regulatory proteins (G proteins) on receptor binding, inhibition of [^{3}H]WEB 2086 binding by agonists, experiments were carried out in the presence of known G protein regulators (Gilman, 1989). For GTP-gamma-S, membranes were incubated with 100 μM GTP-gamma-S in 50 mM Tris buffer containing 5 mM $MgCl_2$, pH 7.4 for 60 min and 25°C, centrifuged, and resuspended in buffer as described above. For pertussis and cholera toxin treatment, membranes were incubated with 25 and 200 μg/ml respectively in 50 mM Tris buffer containing 5 mM $MgCl_2$, 5 mM ATP, pH 7.4, for 60

Figure 7. Rebinding of [^{3}H]C_{16}-PAF to GPLM.

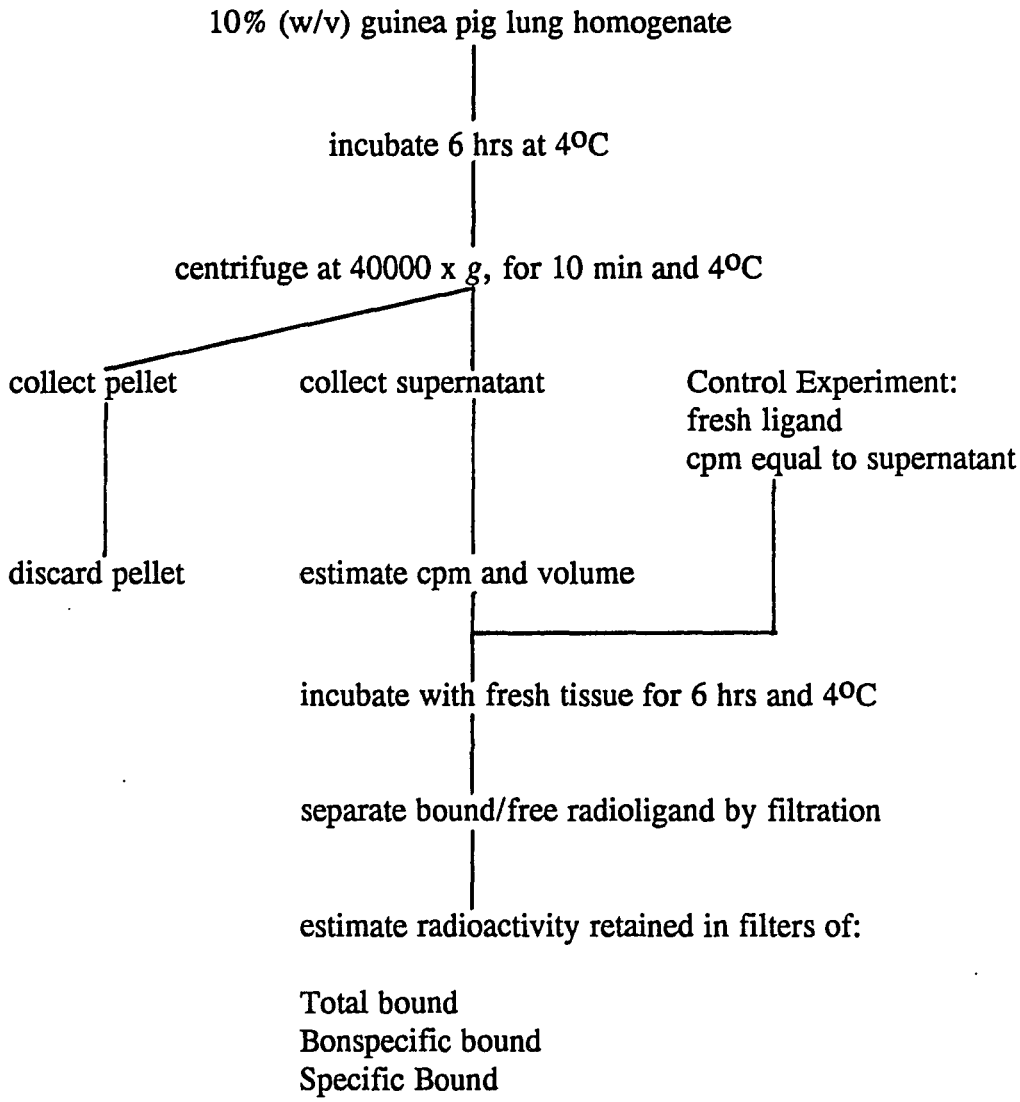

min at 25°C, followed by centrifugation at 40000 x *g* for 15 min and 4°C. The resulting pellet was resuspended in 50 mM Tris, 5 mM $MgCl_2$, buffer at pH 7.4. For PMA treatment, membranes were incubated with 50 ng/ml of PMA in 50 mM Tris buffer containing 5 mM $MgCl_2$, pH 7.4, for 15 min and 25°C, centrifuged and resuspended in buffer as described. For Na^+ treatment, membranes were incubated in 50 mM Tris, 5 mM $MgCl_2$, 150 mM NaCl, pH 7.4 for 60 min and 25°C, centrifuged and resuspended in buffer as described.

Data Analysis

Experimental data for the saturation and inhibition experiments were analyzed using nonlinear least-squares regression by a computerized iterative procedure obtained from Susan Yamamura (Tucson, AZ). All data derived from the saturation and inhibition studies were analyzed for one- and two-site binding models according to the Law of Mass Action by nonlinear least-squares fit as described (23). Data from independent experiments were combined and then fit successively to both one- and two-site models. The residual sum of the squares, a measure of the variability between the fitted and experimentally derived data was used in evaluating the significance of fit for each model as described previously using the partial *F* test (21). IC_{50} values derived from inhibition experiments were converted to

inhibitory constants (K_i) using the Cheng and Prusoff (16) equation. Data derived from kinetic experiments were analyzed using nonlinear least-squares regression analysis (Biosoft, Milltown, NJ). The mean values for log-normally distributed data (k_{+1}, k_{-1}, K_d, IC_{50}, and K_i) are reported as the geometric mean value x/÷ the SEM. The mean values for Bmax, and n_H are reported as the arithmetic mean ± the SEM.

CHAPTER III

RESULTS

Radioligand Binding Studies with [^{3}H]C_{16}-PAF

Kinetic Experiments: Initial experiments revealed specific binding sites for PAF in GPLM and RPM in kinetic studies. Binding of 0.5 nM [^{3}H]C_{16}-PAF achieved plateau levels within 6 hrs at 4°C in both GPLM and RPM, as shown in a representative association experiment (Figure 8). The association rate constant (k_{+1}) determined by pseudo-first order analysis of association data (n=4) was 44.8x10^6 M^{-1} min^{-1} for GPLM and 1.5x10^3 M^{-1} min^{-1} for RPM. For GPLM, dissociation of the ligand receptor complex occurred with $T_{½}$ of 30 x/÷ 1.2 min (geometric mean x/÷ SEM) and a k_{-1} of 0.023 min^{-1}. For RPM, dissociation occurred with a $T_{½}$ of 120.2 x/÷ 1.1 min and a k_{-1} of 0.0057 min^{-1}. Representative dissociation experiments are shown in Figure 9. The kinetic K_d (k_{-1}/k_{+1}) determined from GPLM data was 0.87 x10^{-9} x/÷ 2.4 M (n=4). The kinetic K_d determined for RPM data was 3.6 x10^{-9} x/÷ 1.2 M (n=4).

Saturation Experiments: Saturability of [^{3}H]C_{16}-PAF (0.1 to 20 nM range) in GPLM and RPM is illustrated in Figure 10. In GPLM, total radioligand bound accounted for 4-7% of the total [^{3}H]C_{16}-PAF added. In RPM, total radioligand bound accounted for 0.7-3.5% of the total [^{3}H]C_{16}-PAF added. Nonspecific binding increased linearly

Figure 8A. **GPLM**

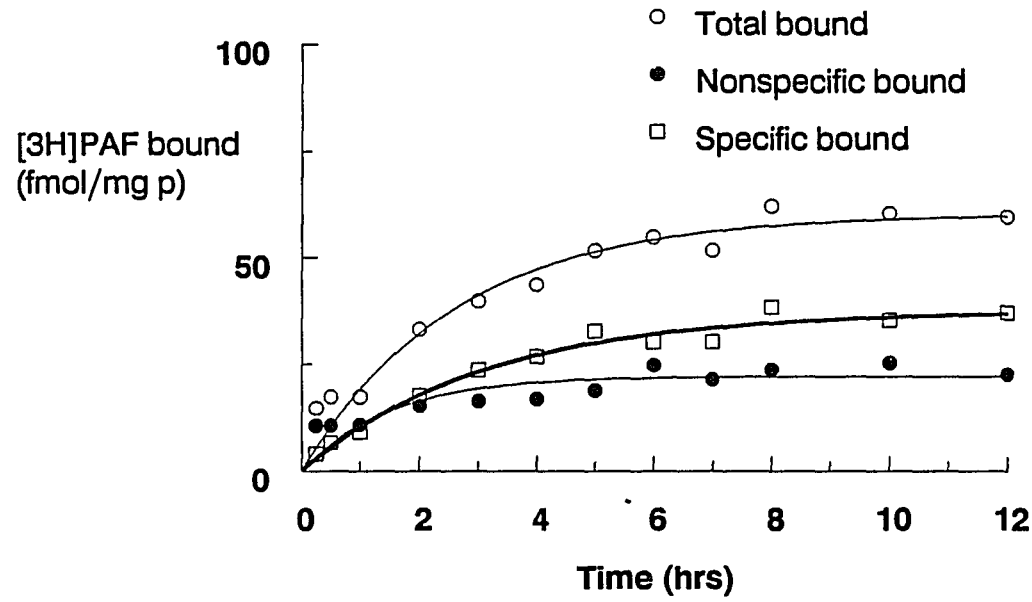

Figure 8B. **RPM**

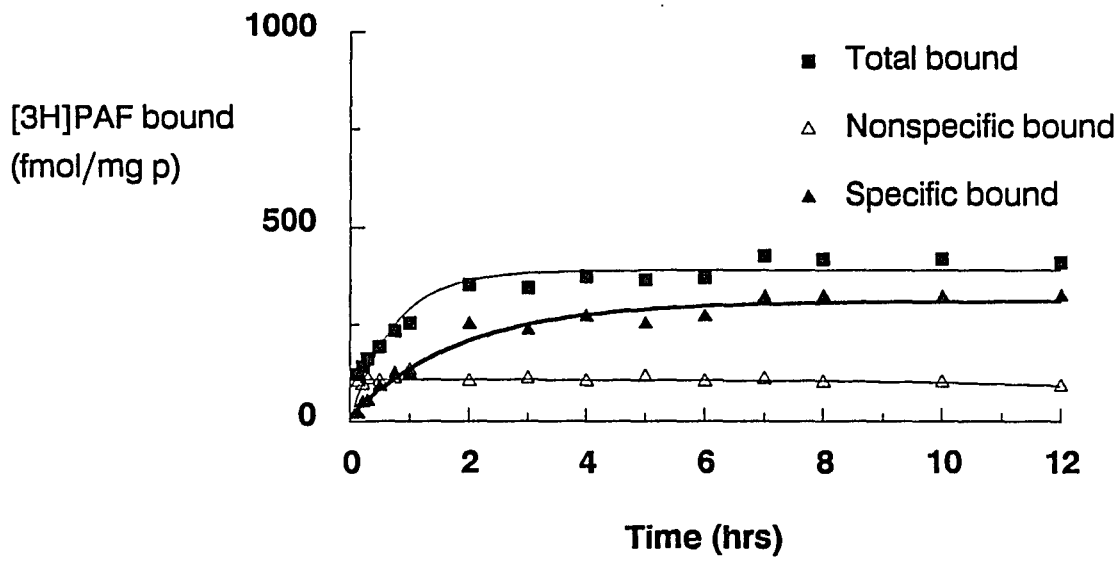

Figure 8. Association of 0.5 nM [^{3}H]C_{16}-PAF binding to GPLM and RPM. Experiments were done in the absence (total bound) and presence (nonspecific bound) of 10^{-4}M WEB2086. Specific bound was determined as the difference between total and nonspecific radioligand bound. The association rate constant for specific bound data was 50.5 x10^6 M^{-1} min^{-1} for GPLM, and 11.3 x10^4 M^{-1} min^{-1} for RPM data.

Figure 9A.

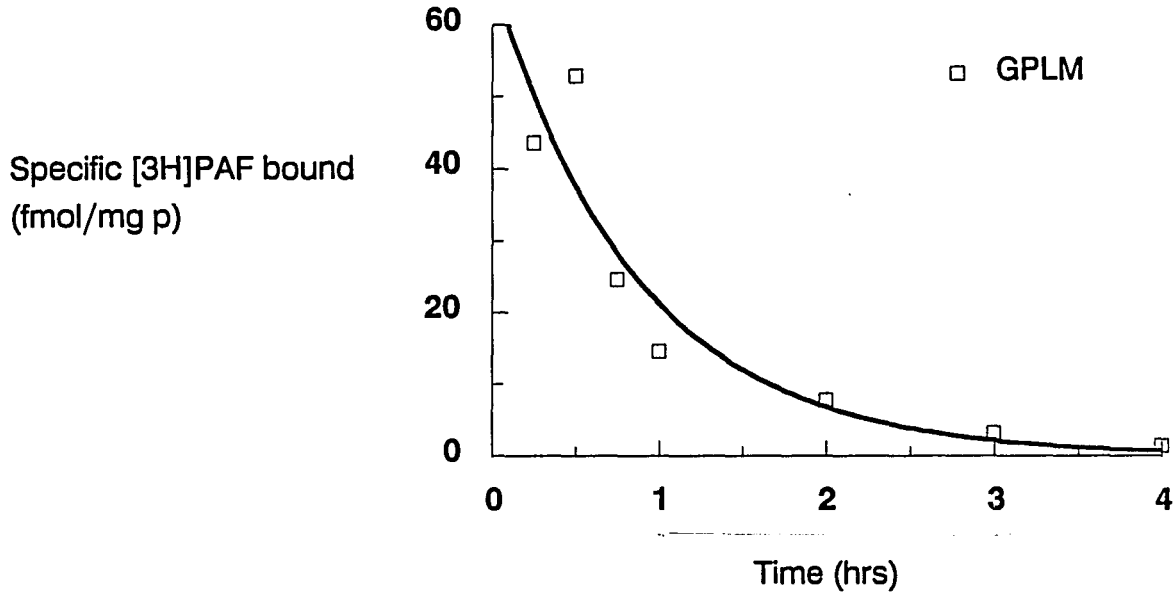

Figure 9B.

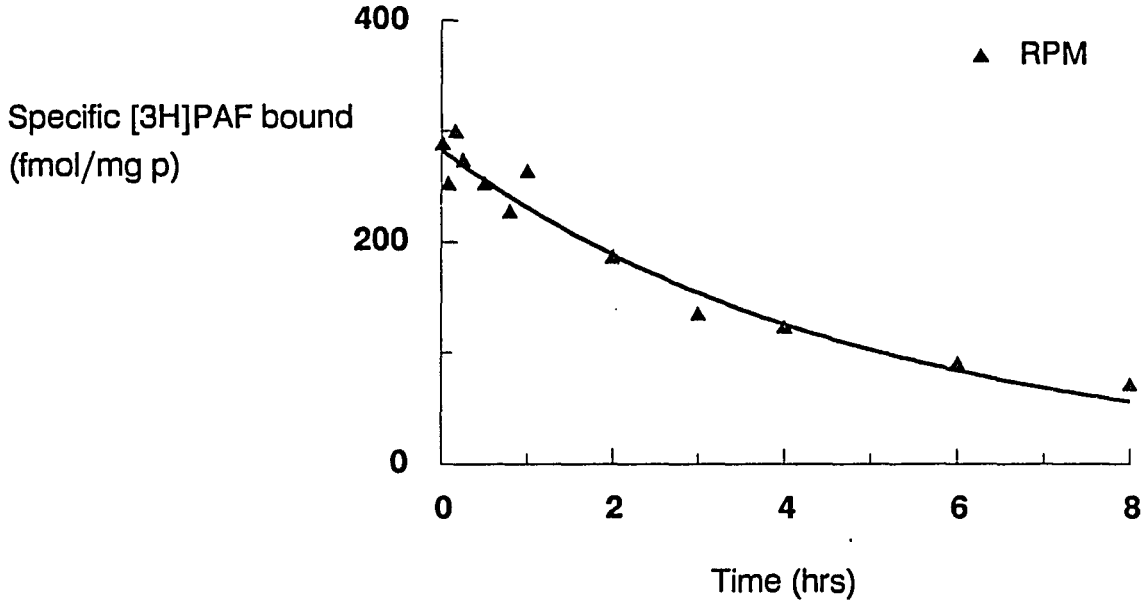

Figure 9. Dissociation of 0.5 nM [^{3}H]C_{16}-PAF binding to GPLM and RPM. The dissociation rate constant for specific binding data in GPLM was 0.012 min^{-1} and T½ of 57 min. The dissociation rate constant for RPM data was 0.0046 min^{-1} and T½ of 150 min.

with increasing concentrations of [^{3}H]C_{16}-PAF in the presence of 10 μM C_{16}-PAF or 100 μM WEB 2086. Binding parameters derived from saturation isotherms are given in Table I. Analysis of saturation data with [^{3}H]C_{16}-PAF were best described by a 1-site fit over the molar concentration range used in both GPLM and RPM. In GPLM, the binding of [^{3}H]C_{16}-PAF was saturable and yielded a K_d of 2.6 x/÷ 1.3 nM, and a Bmax of 200 fmol/mg of protein (*n=6*). In RPM, binding of [^{3}H]C_{16}-PAF yielded a K_d of 1.4 x/÷ 1.3 nM and a Bmax of 1922 fmol/mg protein (*n=5*). In both GPLM and RPM, the Hill slope was near unity (1.0 and 0.9, respectively).

Inhibition Experiments: The pharmacological specificity of [^{3}H]C_{16}-PAF binding to GPLM and RPM was examined by comparing the inhibitory potencies of the PAF species C_{16}-PAF, C_{18}-PAF, and C_{16}-lyso-PAF (shown in Figure 11) and the PAF antagonists WEB 2086 and RP52770 (Figure 12). Specific binding of 0.5 nM [^{3}H]C_{16}-PAF was inhibited in a dose-dependent manner and to the same extent (50% in GPLM and 75% in RPM) by C_{16}-PAF, C_{18}-PAF, WEB 2086, and RP52770. The K_i values derived from these data and pseudo-Hill slopes (n_H) are listed in Table II for GPLM and Table III for RPM.

In GPLM, inhibition of [^{3}H]C_{16}-PAF binding by C_{16}-PAF, C_{18}-PAF, WEB 2086, and RP52770 were best described by a one-site fit (illustrated in Table II). The K_i values for C_{16}-

PAF and WEB 2086 (7 and 27 nM, respectively) were not significantly different from the K_d values derived from saturation data (3 nM for [^{3}H]C_{16}-PAF and 40 nM for [^{3}H]WEB 2086, Table I). In contrast, lyso-PAF failed to inhibit the specific binding of [^{3}H]C_{16}-PAF (GPLM; Figure 11A). As illustrated in Table III, inhibition of binding of [^{3}H]C_{16}-PAF to RPM by C_{16}-PAF, C_{18}-PAF, WEB 2086 and RP52770 were best described by a one-site fit. The K_i values for C_{16}-PAF and WEB 2086 (1 nM for C_{16}-PAF and 20 nM for WEB 2086) were not significantly different from the K_d values obtained from direct saturation experiments (1 nM for [^{3}H]C_{16}-PAF and 41 nM for [^{3}H]WEB 2086, Table I).

Figure 10A. **GPLM**

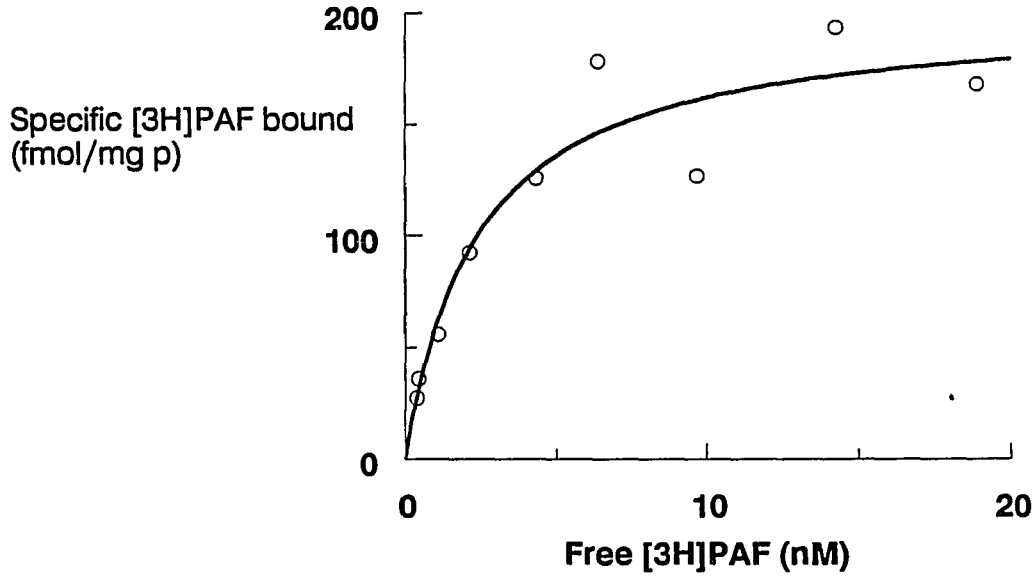

Figure 10B. **RPM**

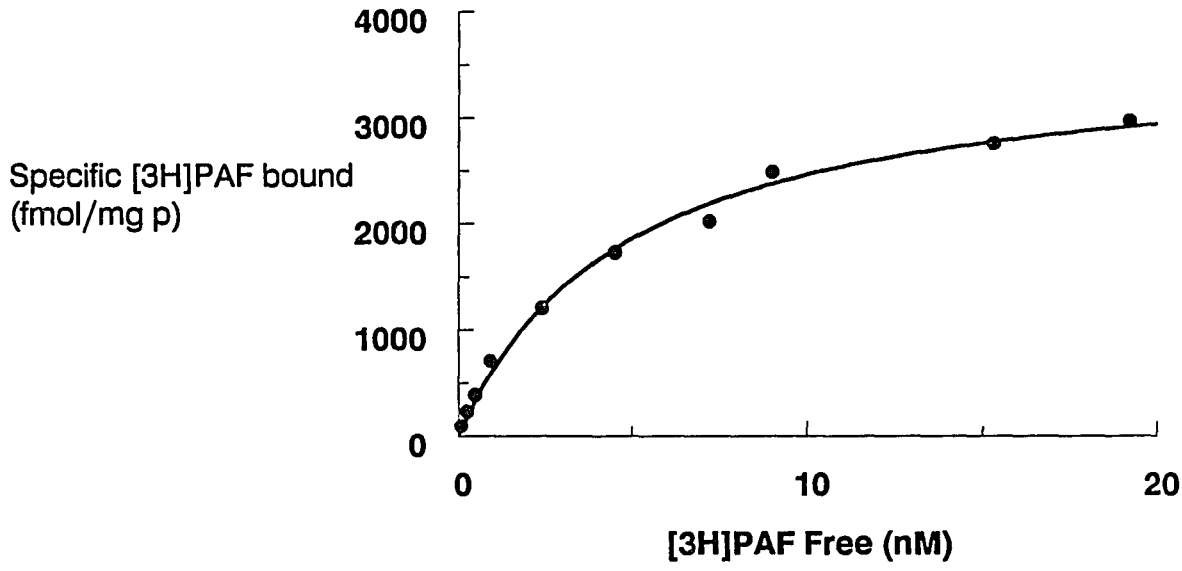

Figure 10. Saturation isotherm of [^{3}H]C_{16}-PAF binding to GPLM and RPM. Specific [^{3}H]C_{16}-PAF bound was determined experimentally as the difference between total and nonspecific bound in parallel assays in the absence and presence of 100 μM WEB 2086. Nonlinear regression analysis of the saturation data gave dissociation constatnt (K_d) of 2.5 nM and a Bmax of 178 fmol/mg protein for GPLM data. The K_d for saturation data in RPM was 4.8 nM and Bmax of 2970 fmol/mg protein.

TABLE I. Binding characteristics of [^{3}H]C_{16}-PAF, [^{3}H]WEB2086, and [^{3}H]RP52770 binding to guinea pig and rabbit platelet membranes.

Membrane	Radioligand	K_d* (nM)	Bmax** (fmol/mg of protein)	Hill Co.**	n
GPLM	[^{3}H]C_{16}-PAF	3 (1.3)	200 (10)	1.0 (0.1)	6
	[^{3}H]WEB2086	40 (1.2)	226 (29)	1.1 (0.1)	4
	[^{3}H]RP52770	42 (1.4)	1620 (185)	1.0 (0.03)	3
RPM	[^{3}H]C_{16}-PAF	1 (1.3)	1922 (964)	0.9 (0.03)	5
	[^{3}H]WEB2086	41 (1.3)	2639 (778)	1.0 (0.02)	5
	[^{3}H]RP52770	36 (2.0)	10105 (2284)	1.1 (0.04)	3

* For each radioligand, K_d values represent the geometric mean with geometric SEM in parenthesis.

**Values for Bmax and Hill coefficients represent the arithmetic mean ± SEM.

Figure 11A. **GPLM**

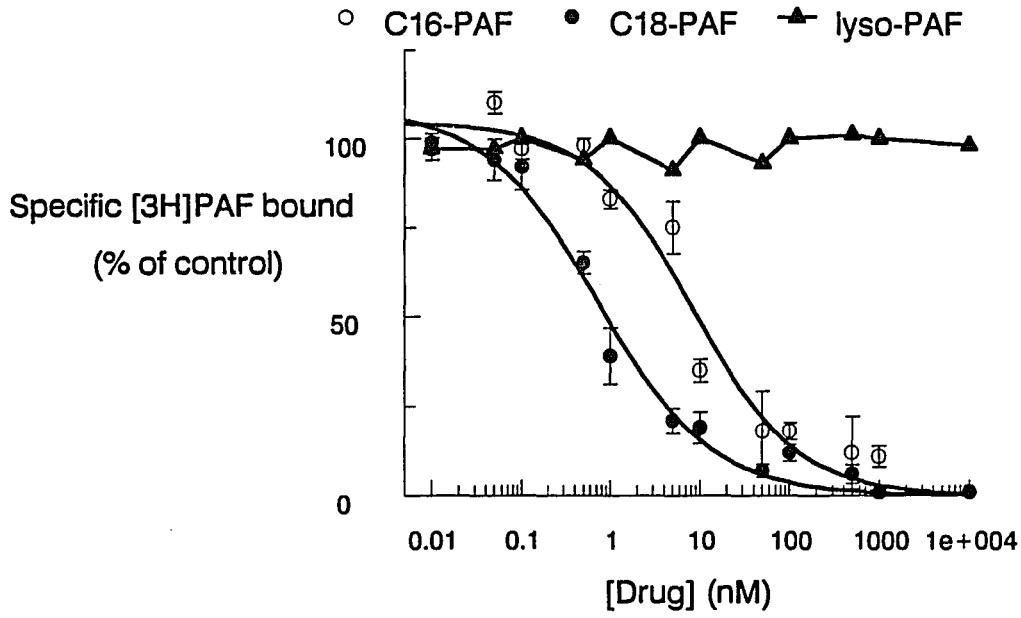

Figure 11B. **RPM**

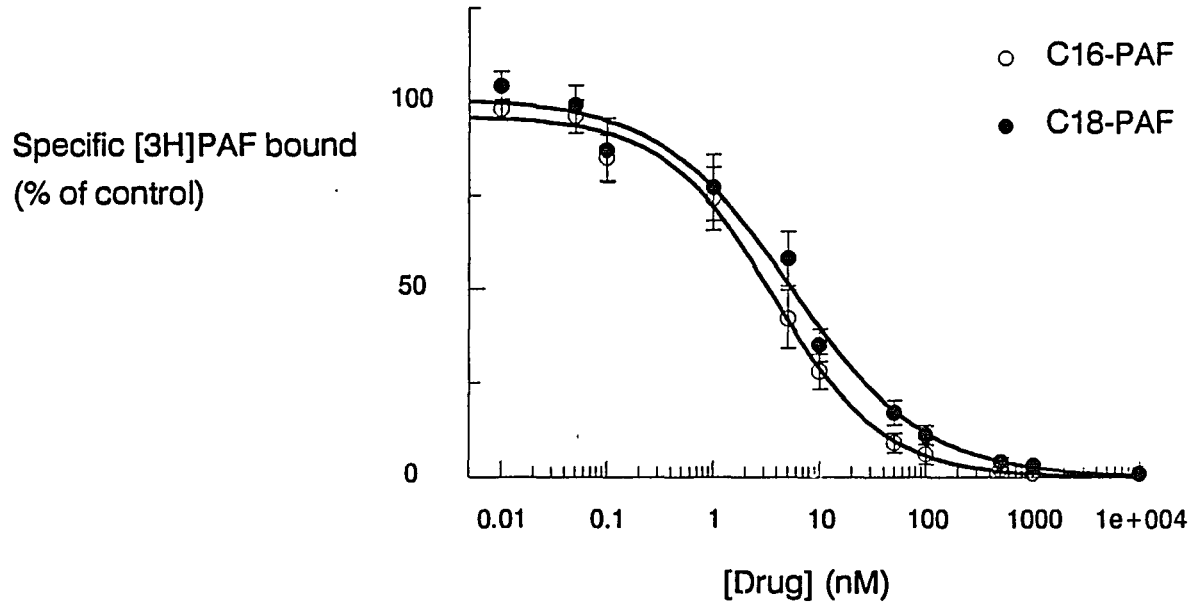

Figure 11. Inhibition of specific [^{3}H]C_{16}-PAF (0.5 nM) binding to GPLM and RPM by agonists. Each data poin represent the mean values (± SEM) of at least 4 separate experiments. Pseudo-Hill slopes and K_i values are listed in Table II for GPLM data, and Table III for RPM data.

Figure 12A. **GPLM**

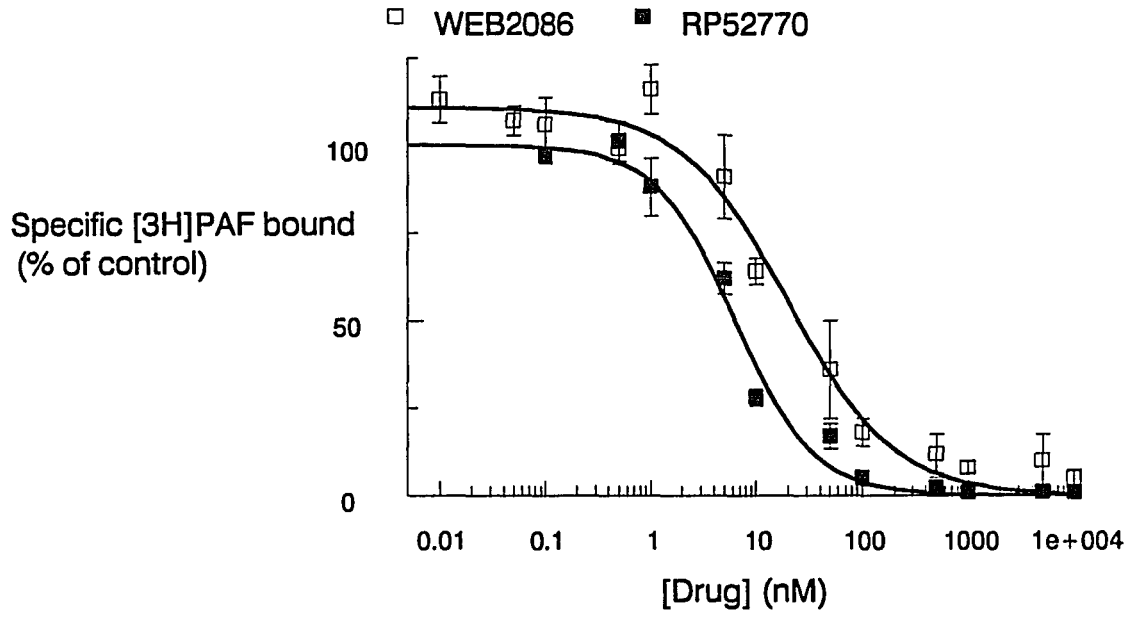

Figure 12B. **RPM**

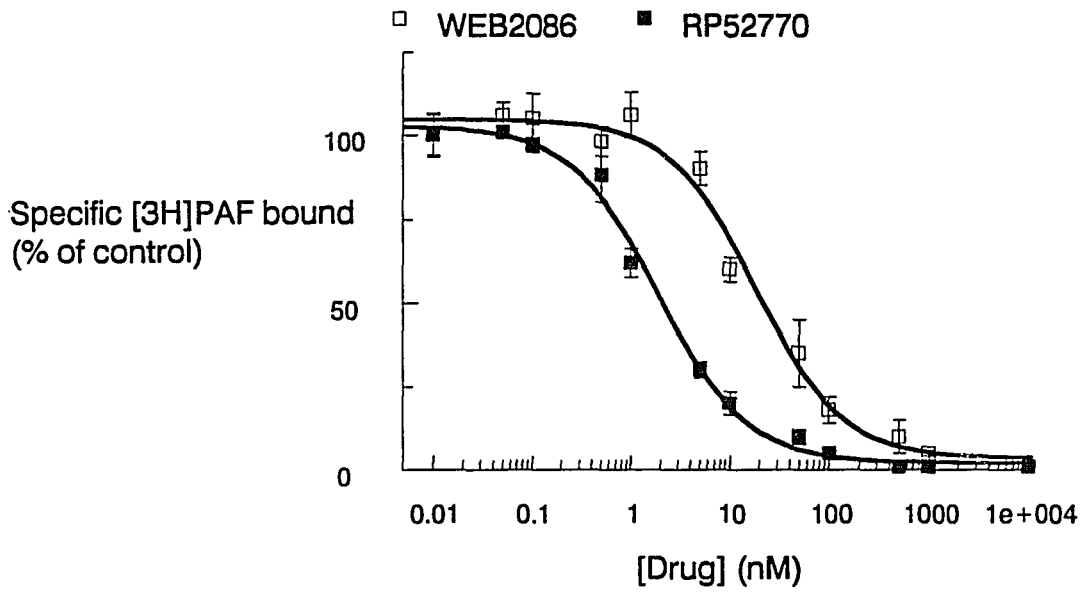

Figure 12. Inhibition of specific [^{3}H]C_{16}-PAF (0.5 nM) binding to GPLM and RPM by antagonists. Data points represent the mean values (± SEM) of 6 separate experiments. Pseudo-Hill slopes and K_i values are given in Table II for GPLM data, and Table III for RPM data.

TABLE II. Inhibition of [^{3}H]C_{16}-PAF and [^{3}H]WEB2086 binding to guinea pig lung membranes by PAF and antagonists.

	[^{3}H]C_{16}-PAF			[^{3}H]WEB2086					
				1-site model		2-site model*			
Unlabeled	K_i**	n_H§	n	K_i	n_H	K_H	%B_H	K_L	n
C_{16}-PAF	7	0.9	8	5	0.6	1	71	416	16
	(1.4)	(0.1)		(1.3)	(0.1)	(2.1)	(4)	(1.6)	
C_{18}-PAF	2	0.9	8	6	0.6	1	72	288	13
	(1.3)	(0.1)		(1.2)	(0.1)	(2.1)	(3)	(2.0)	
WEB2086	27	1.1	8	18	1.0				8
	(1.1)	(0.1)		(1.0)	(0.1)				
RP52770	7	1.0	6	7	1.0				6
	(1.3)	(0.1)		(1.3)	(0.1)				
lyso-PAF	>10000		6	>10000					4

* Data were best fitted by a 2-site model, where K_H (nM) denotes the inhibitory constant for the high affinity site, %B_H is the percentage of radioligand bound to the high affinity site, and K_L denotes the inhibitory constant to the low affinity site.

** Inhibitory constant values were calculated using the Cheng and Prusoff formula and represent the geometric mean x/÷ SEM (in parenthesis).

§ n_H Values represent the arithmetic mean of the pseudo-Hill slope ± SEM (in parenthesis).

TABLE III. Inhibition of [^{3}H]C_{16}-PAF and [^{3}H]WEB2086 binding to rabbit platelet membranes by PAF and antagonists.

	[^{3}H]C_{16}-PAF			[^{3}H]WEB2086					
				1-site model		2-site model*			
Unlabeled	K_i**	n_H§	n	K_i	n_H	K_H	%B_H	K_L	n
C_{16}-PAF	1	0.9	8	2	0.6	2	76	214	10
	(1.1)	(0.5)		(1.4)	(0.1)	(1.4)	(6)	(2.7)	
C_{18}-PAF	2	0.8	8	4	0.7	2	65	263	6
	(1.2)	(0.5)		(1.6)	(0.1)	(1.9)	(8)	(2.9)	
WEB2086	20	0.9	4	24	1.0				4
	(1.1)	(0.1)		(1.3)	(0.1)				
RP52770	2	1.0	4	10	1.0				4
	(1.2)	(0.1)		(1.1)	(0.1)				
lyso-PAF	>10000		4	>10000					4

* Data were best fitted by a 2-site model, where K_H (nM) denotes the inhibitory constant for the high affinity site, %B_H is the percentage of radioligand bound to the high affinity site, and K_L denotes the inhibitory constant to the low affinity site.

** Inhibitory constant values were calculated using the Cheng and Prusoff formula and represent the geometric mean x/÷ SEM (in parenthesis).

§ n_H Values represent the mean of the pseudo-Hill slopes ± SEM (in parenthesis).

Radioligand Binding Studies with [^{3}H]WEB 2086

Kinetic Experiments: Direct radioligand binding studies were carried out with [^{3}H]WEB 2086. Steady-state binding of [^{3}H]WEB 2086 (7 nM) was observed within three hrs at 4°C in both GPLM and RPM as shown in Figure 13. The k_{+1} derived from pseudo-first order analysis of association data was 3.7 x 10^5 M^{-1} min^{-1} for GPLM (n=4) and 1.6 x 10^4 M^{-1} min^{-1} for RPM (n=4). Dissociation of [^{3}H]WEB 2086 binding to GPLM and RPM is shown in Figure 14. In GPLM, the $T_{½}$ derived from dissociation data was 22 x/÷ 1.7 min and the k_{-1} value was 0.029 min^{-1}. In RPM the $T_{½}$ was 120 x/÷ 1.3 min and the k_{-1} value was 0.0057 min^{-1}. The kinetic K_d derived from these rate constants were 8 x/÷ 1.4 nM for GPLM, and 35 x/÷ 1.3 nM for RPM.

Saturation Experiments: Saturability of GPLM and RPM by [^{3}H]WEB 2086 (5 to 200 nM range) is shown in Figure 15 and binding parameters are given in Table I. In GPLM, total radioligand bound accounted for 0.4-0.7% of the total radioligand added, where in RPM it accounted for 0.1-0.3% of the total radioligand added. The Bmax values for binding sites labeled by [^{3}H]C_{16}-PAF and [^{3}H]WEB 2086 were not significantly different (GPLM: $p>0.1$; RPM $p>0.1$). In addition, the Bmax values labeled by [^{3}H]WEB 2086 were not significantly different when 10 μM C_{16}-PAF or 100 μM WEB 2086 were used for nonspecific binding (n=4). These

Figure 13A. **GPLM**

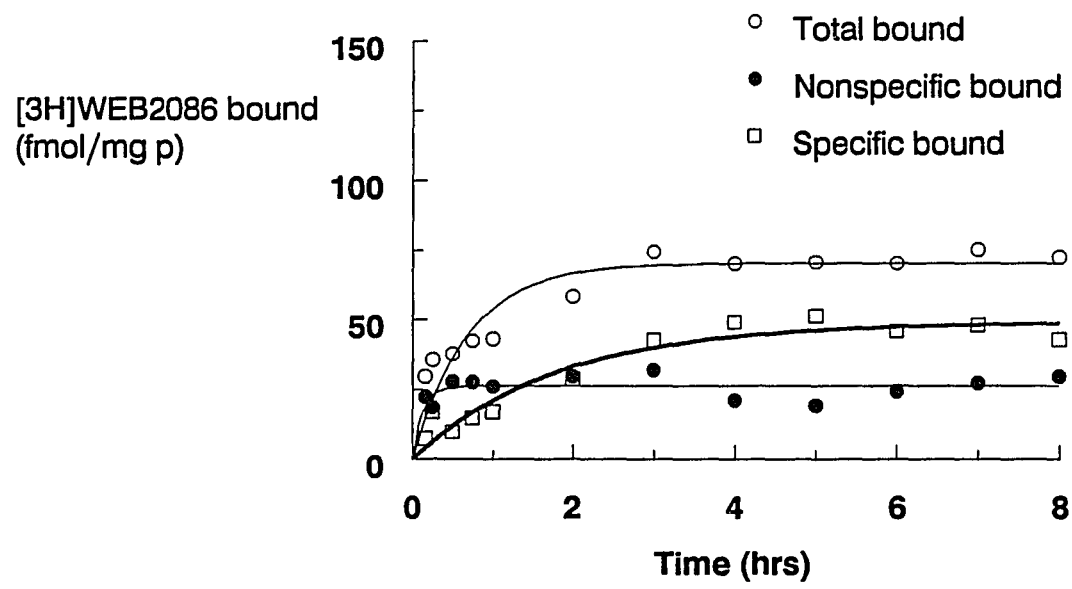

Figure 13B. **RPM**

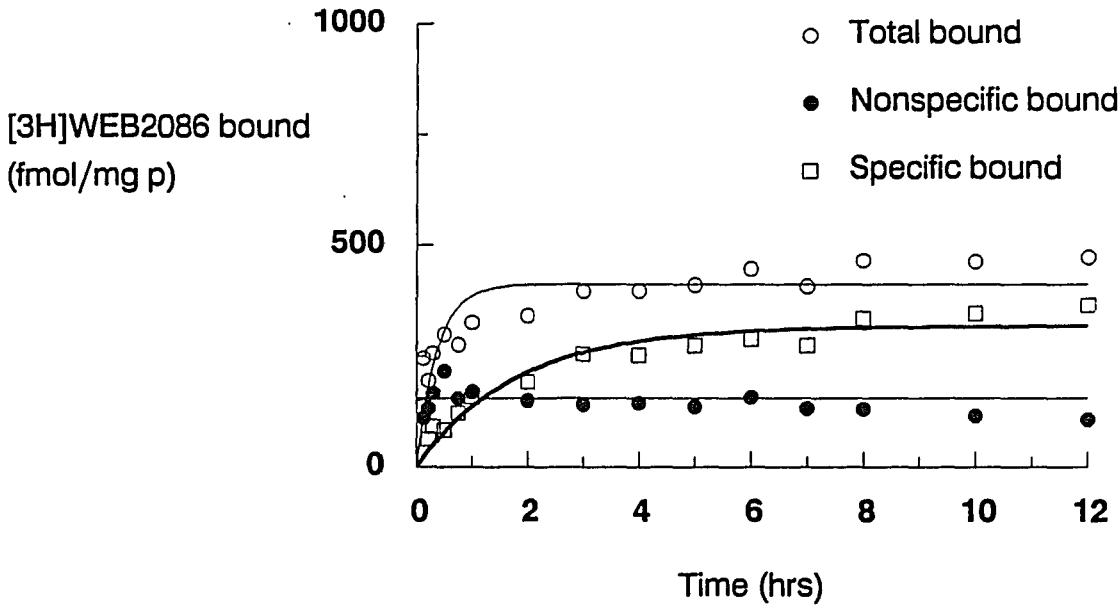

Figure 13. Association of 5 nM [^{3}H]WEB2086 binding to GPLM and RPM. Experiments were carried out in the absence and presence of 10^{-4}M WEB 2086. Specific bound was determined as the difference between total and nonspecific radioligand bound. The association rate constant for specific bound data was 2.22 x10^6 M^{-1} min^{-1} for GPLM, and 14.2 x10^5 M^{-1} min^{-1} for RPM data.

Figure 14A.

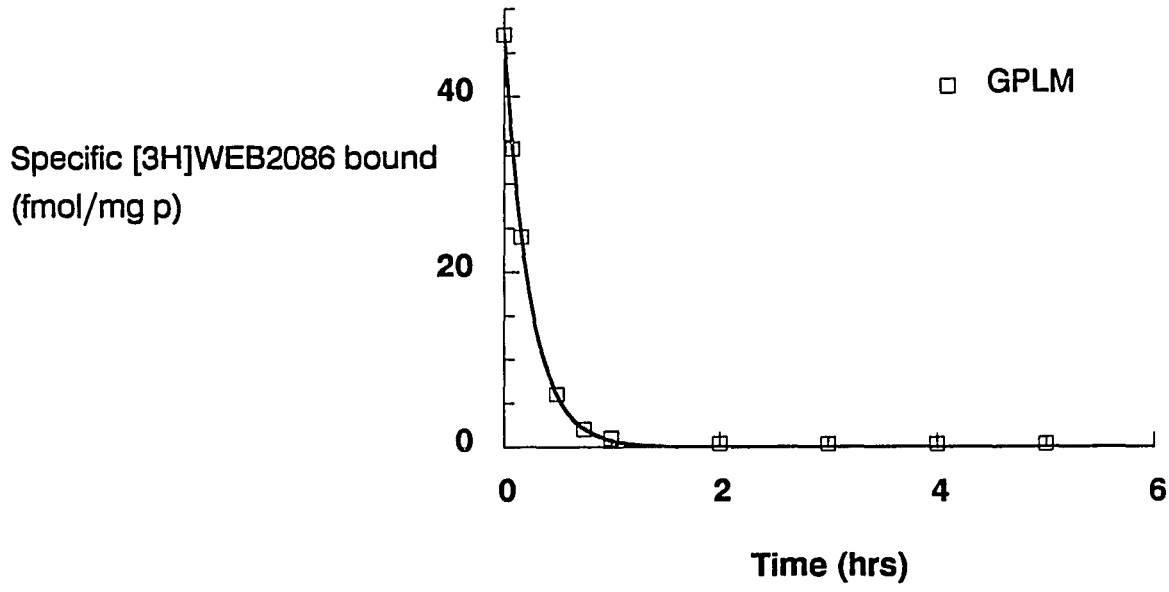

Figure 14B.

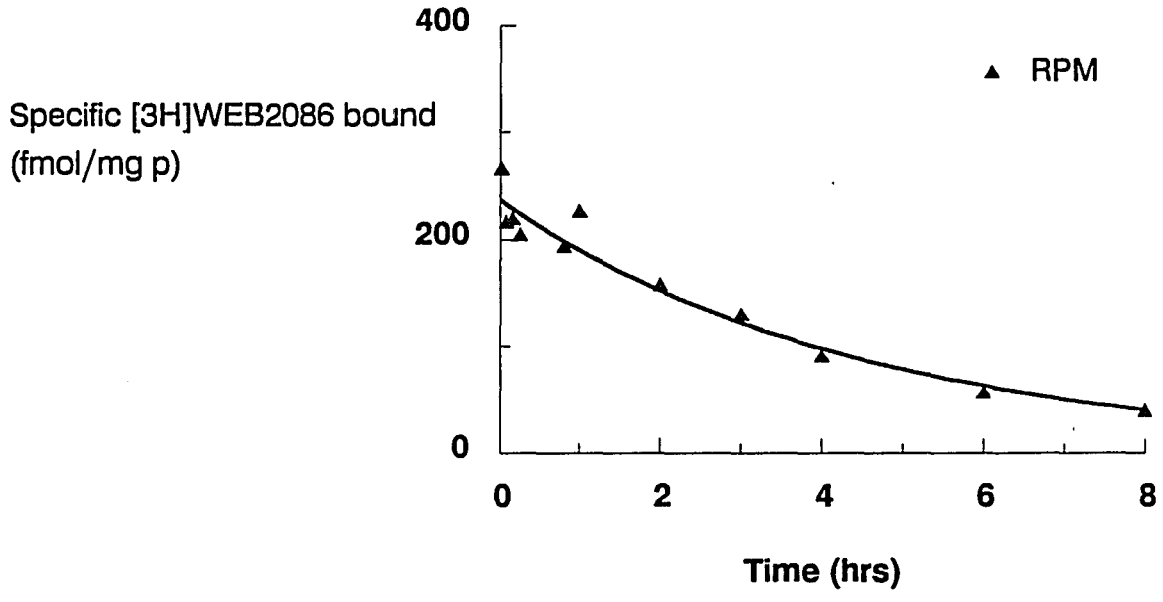

Figure 14. Dissociation of 5 nM [^{3}H]WEB 2086 binding to GPLM and RPM. The dissociation rate constant for specific binding data in GPLM was 0.03 min^{-1} and a T½ of 21 min. The dissociation rate constant for specific binding in RPM was 0.004 min^{-1} and a T½ of 150 min.

Figure 15A. **GPLM**

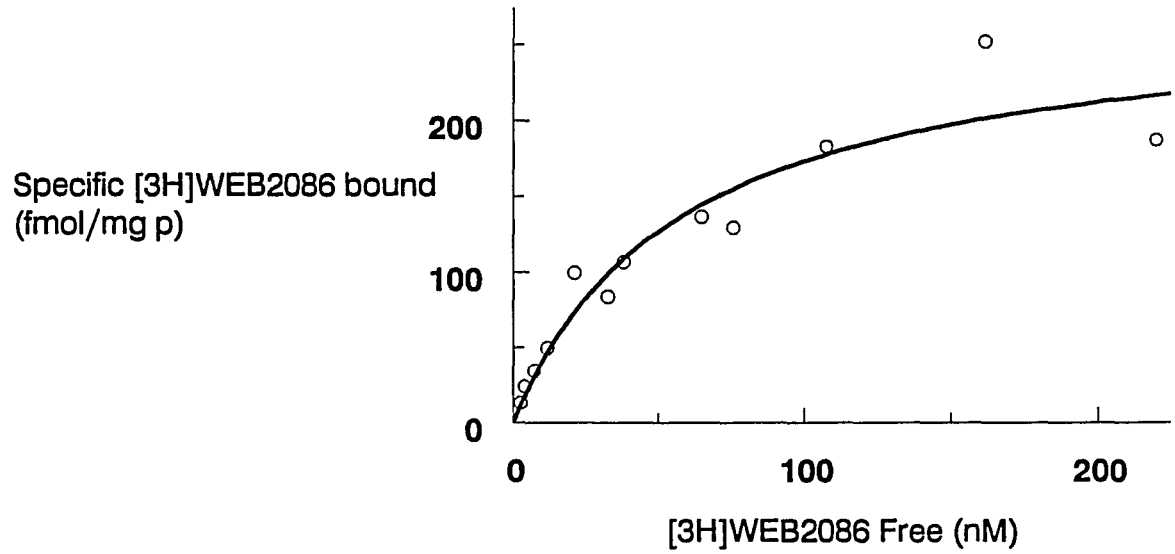

Figure 15B. **RPM**

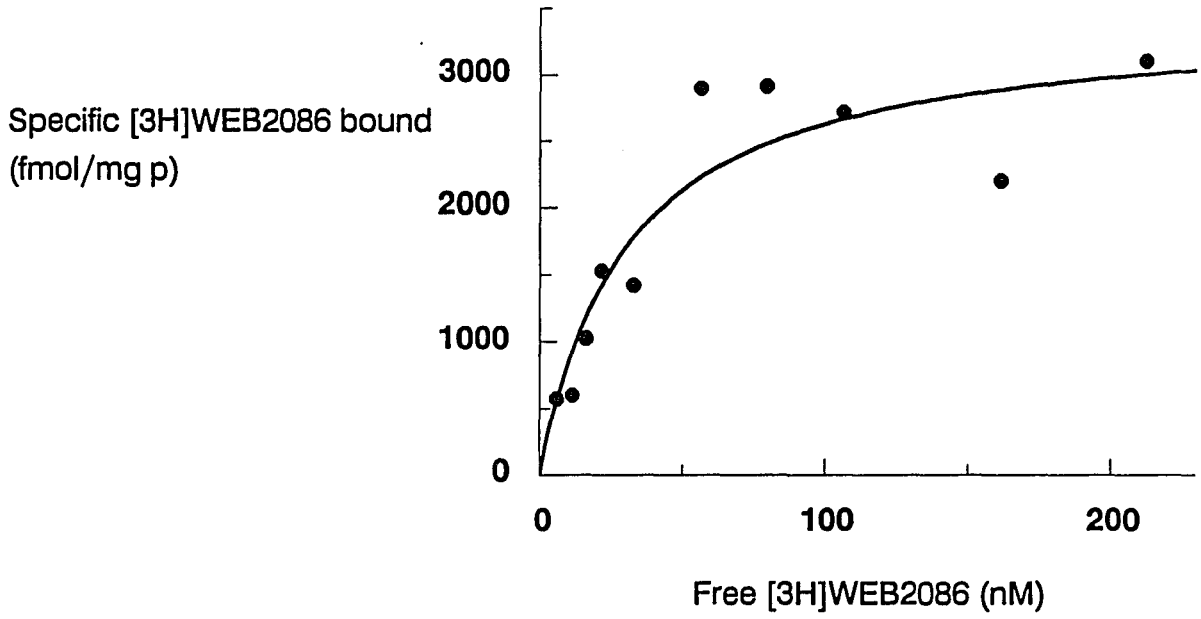

Figure 15. Saturation isotherm of [^{3}H]WEB2086 binding to GPLM and RPM. Nonlinear regression analysis of the saturation data yielded a K_d of 50 nM and a Bmax of 220 fmol/mg of protein for GPLM. The K_d for saturation data in RPM was 30 nM and a Bmax of 3000 fmol/mg of protein.

observations indicate that [^{3}H]WEB 2086 interacts with approximately the same number of receptor sites as [^{3}H]C_{16}-PAF and appears to interact at the same sites. Analysis of saturation data using [^{3}H]WEB 2086 were best described by a 1-site fit in both GPLM and RPM. In GPLM, [^{3}H]WEB 2086 binding was saturable and yielded a K_d of 40 x/÷ 1.2 nM and a Bmax of 226 fmol/mg of protein (*n=4*). In RPM, [^{3}H]WEB 2086 binding was saturable and yielded a K_d of 41 x/÷ 1.3 nM, and a Bmax of 2639 fmol/mg of protein (*n=5*). In both tissue preparations the Hill slopes were near unity (GPLM=1.1, RPM=1.0) over the molar concentration range of radioligand used.

Inhibition Experiments: The pharmacological specificity of [^{3}H]WEB 2086 binding to GPLM and RPM was examined by comparing the inhibitory potencies of the PAF species C_{16}-PAF, C_{18}-PAF, lyso-PAF (Figure 16), and the PAF antagonists WEB 2086 and RP52770 (Figure 17). Specific binding of 7 nM [^{3}H]WEB 2086 was inhibited in a dose-dependent manner and to the same extent by all the unlabeled drugs except lyso-PAF. The K_i values of inhibition data are given in Table II and III for GPLM and RPM data, respectively. The inhibition curves for C_{16}-PAF and C_{18}-PAF in competition with [^{3}H]WEB 2086 were shallow (Figure 16) and statistically better described by a two-site rather than one-site model (partial F test $p<0.05$) in both GPLM and RPM.

Figure 16A.

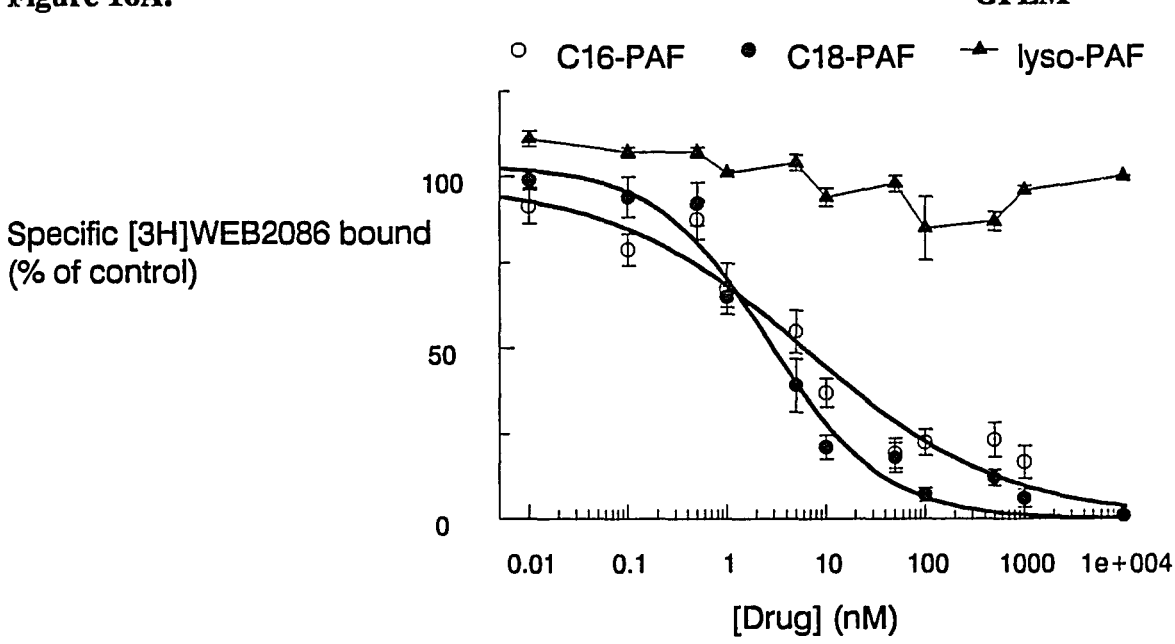

Figure 16B.

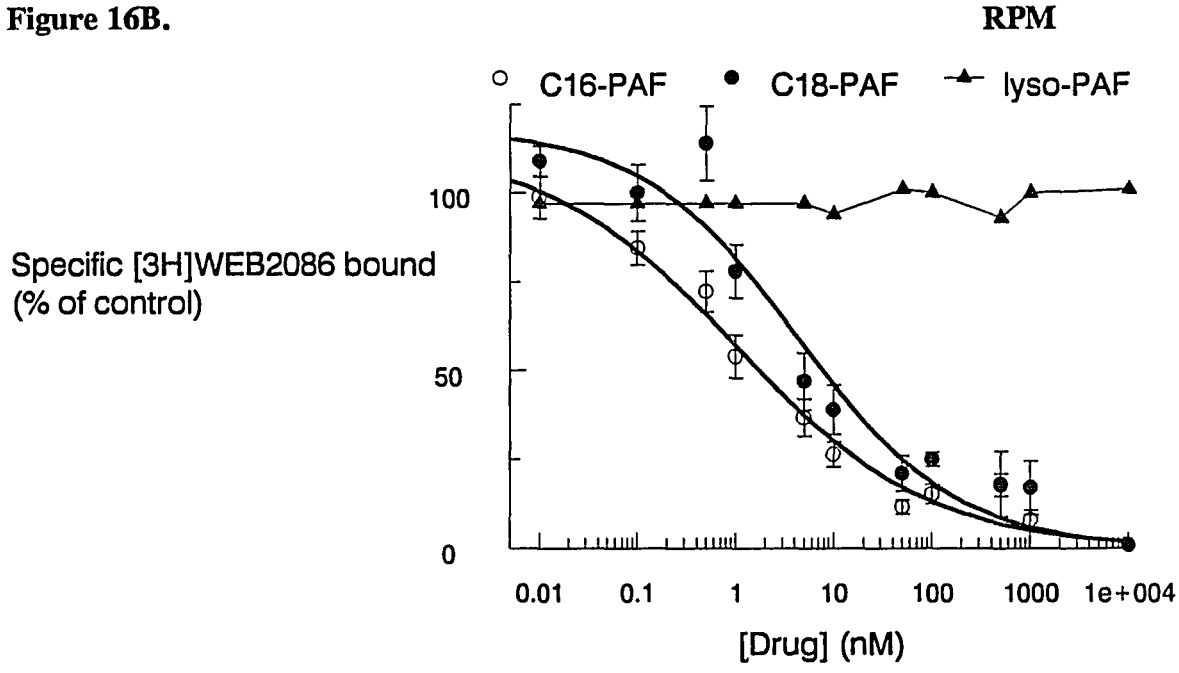

Figure 16. Inhibition of specific [^{3}H]WEB2086 (7 nM) binding to GPLM and RPm by agonists. Each data point represent the mean (± SEM) of at least 4 separate experiments. Pseudo-Hill slopes and K_i values are listed in Table II for GPLM, and Table III for RPM data.

Figure 17A.

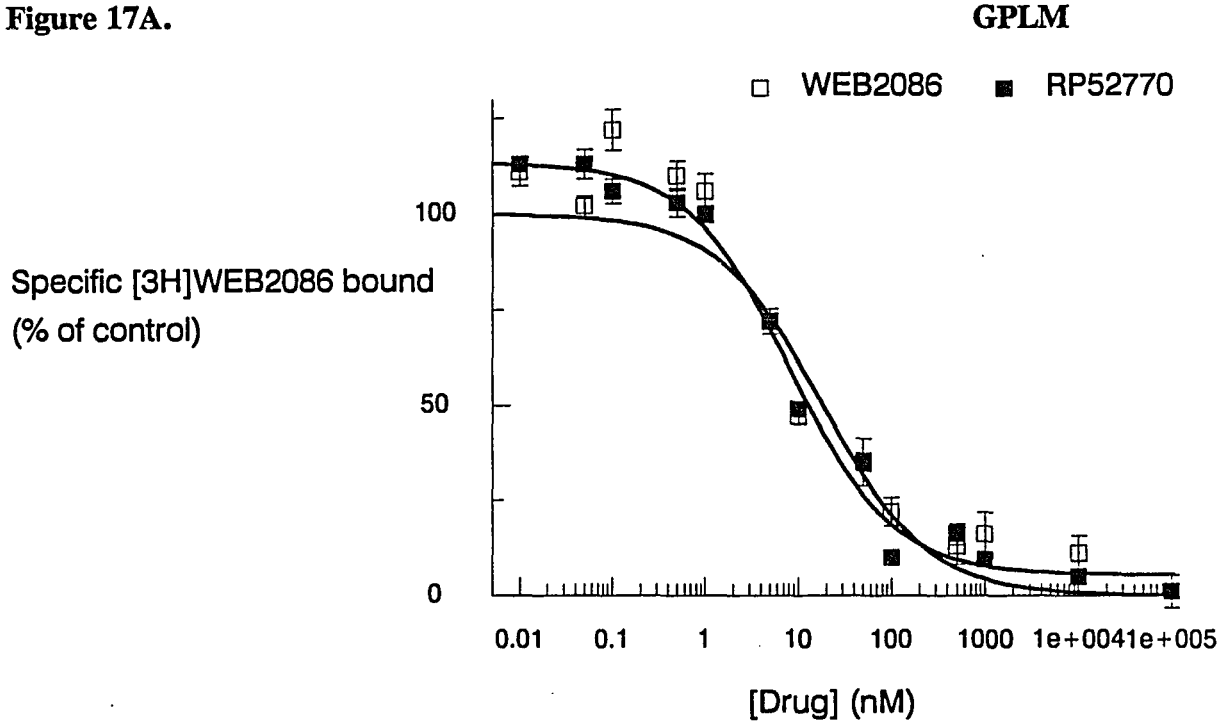

Figure 17B.

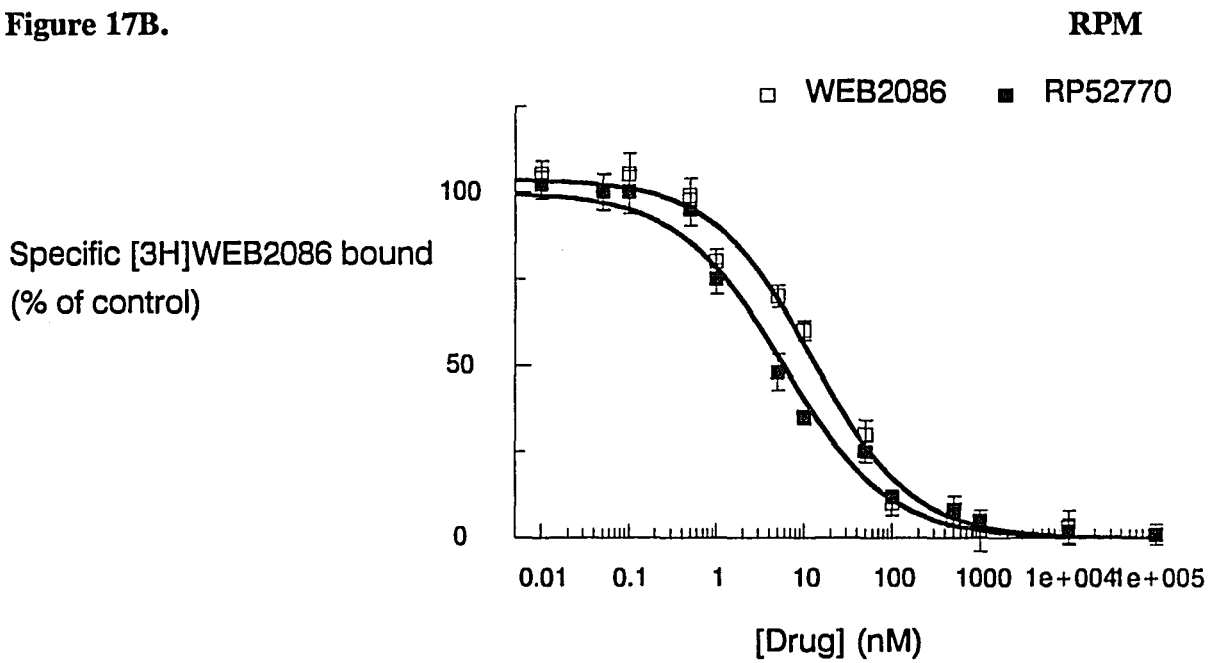

Figure 17. Inhibition of specific [^{3}H]WEB2086 (7 nM) binding to GPLM and RPM by antagonists. Pseudo-Hill coefficients and K_i values are given in Table II for GPLM data and Table III for RPM data.

Transformation of C_{16}-PAF and C_{18}-PAF inhibition data in GPLM yielded pseudo-Hill slopes of 0.6 in both cases. These results are summarized in Table II where the estimated K_i values for the high and low affinity are termed K_H and K_L, respectively. The high affinity for C_{16}-PAF comprised 71% of the total receptor population with a K_i of 1 nM and the low affinity yielded a K_i of 416 nM (*n=16*). The high affinity for C_{18}-PAF comprised 72% of the total receptor population with a K_i of 1.2 nM and the low affinity yielded a K_i of 288 nM (*n=11*). In contrast, inhibition of [^{3}H]WEB 2086 binding by the PAF antagonists WEB 2086 and RP52770 yielded steep inhibition curves with pseudo-Hill slopes of 1.0 (Figure 17A and Table II).

Results from inhibition of [^{3}H]WEB 2086 binding data in RPM are summarized in Table III. Transformation of C_{16}-PAF and C_{18}-PAF inhibition data yielded pseudo-Hill slopes of 0.6 and 0.7 respectively. The high affinity for C_{16}-PAF comprised 76% of the total receptor population with a K_i of 2 nM and the low affinity yielded a K_i of 214 nM (*n=10*). The high affinity for C_{18}-PAF in RPM comprised 65% of the total receptor population with a K_i of 1.5 nM and the low affinity yielded a K_i of 263 nM (*n=6*). In contrast, the PAF antagonists WEB 2086 and RP52770 inhibited the binding of [^{3}H]WEB 2086 yielding steep inhibition curves (Figure 17B and Table III) and pseudo-Hill slopes of unity (*n=4*).

Radioligand Binding Studies with [^{3}H]RP52770.

Saturation Experiments: Saturation isotherm experiments using [^{3}H]RP52770 in GPLM yielded a K_d of 42 x/÷ 1.4 nM, and a Bmax of 1620 fmol/mg of protein (*n=3*), a binding site density 8-fold greater than that obtained with [^{3}H]C_{16}-PAF and [^{3}H]WEB 2086 (Figure 18A and Table I). In RPM, saturation experiments with [^{3}H]RP52770 yielded a K_d of 36 x/÷ 2.0 nM, and a Bmax of 10105 fmol/mg of protein (*n=3*) a binding site density 5-fold greater than that obtained with [^{3}H]C_{16}-PAF and [^{3}H]WEB 2086 (see Table I). These data yielded Hill coefficients of unity for both GPLM and RPM data.

Inhibition Experiments: As shown in Figure 19A, specific binding of 7 nM [^{3}H]RP52770 to GPLM was inhibited by unlabeled RP52770 (90% of the control) and yielded a K_i of 35 nM. However, neither the PAF species C_{16}-PAF, C_{18}-PAF, C_{16}-lyso-PAF nor the PAF antagonist WEB 2086 inhibited the specific binding of [^{3}H]RP52770 (*n=4*). In contrast to the binding in GPLM, [^{3}H]RP52770 binding to RPM (shown in Figure 19B) was inhibited by unlabeled RP52770 only to 50% of the control. The K_i derived from these experiments was 95 x/÷1.2 nM (*n=4*). In addition, C_{16}-PAF, C_{18}-PAF and WEB 2086 inhibited binding to 30% of the control (*n=3*). The estimated K_i's for these inhibition curves were (in nM) 200

Figure 18A. **GPLM**

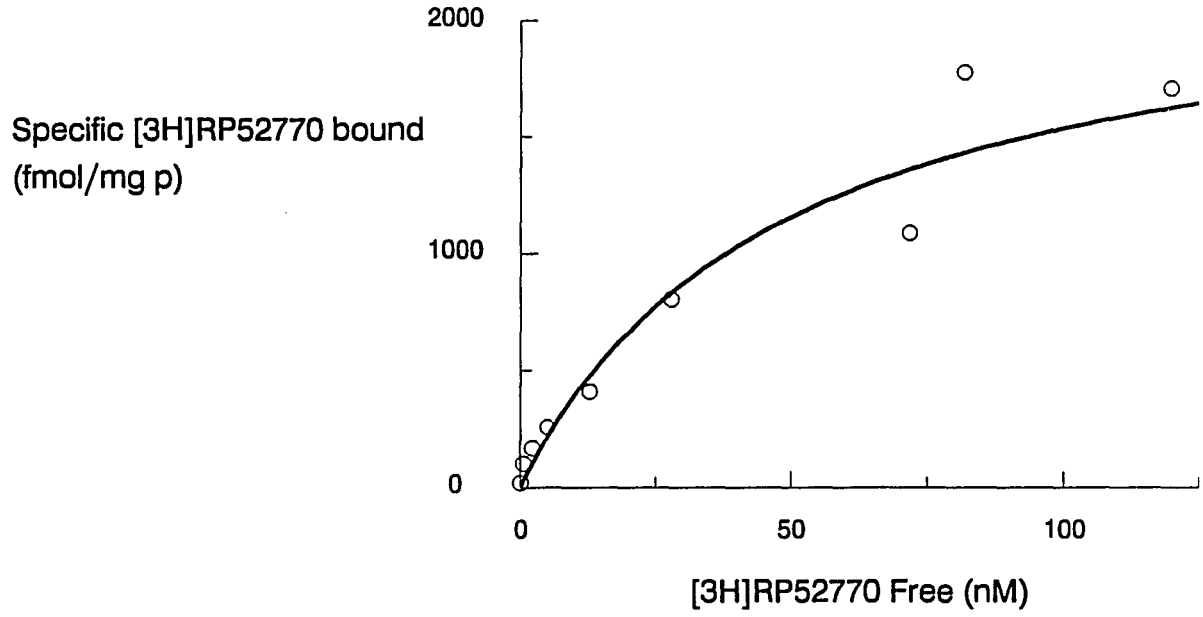

Figure 18B. **RPM**

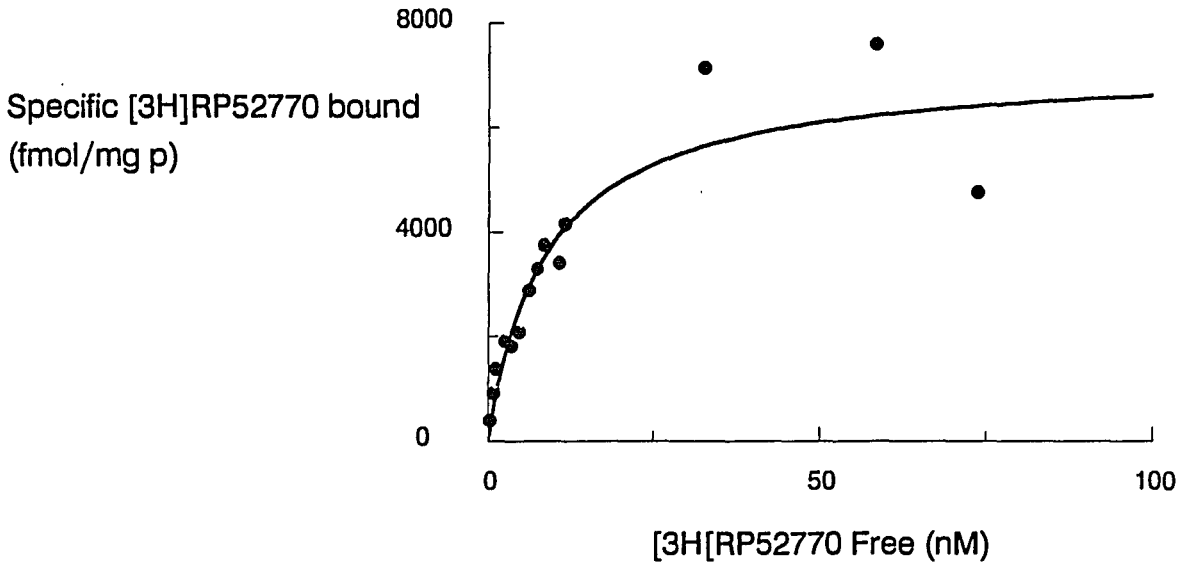

Figure 18. Saturation isotherms of [^{3}H]RP52770 binding to GPLM and RPM. Nonlinear regression analysis of saturation data yielded a K_d of 35 nM and a Bmax of 1800 fmol/mg of protein for GPLM data. The K_d for saturation data in RPM was 15 nM and a Bmax of 6500 fmol/mg protein.

Figure 19A.

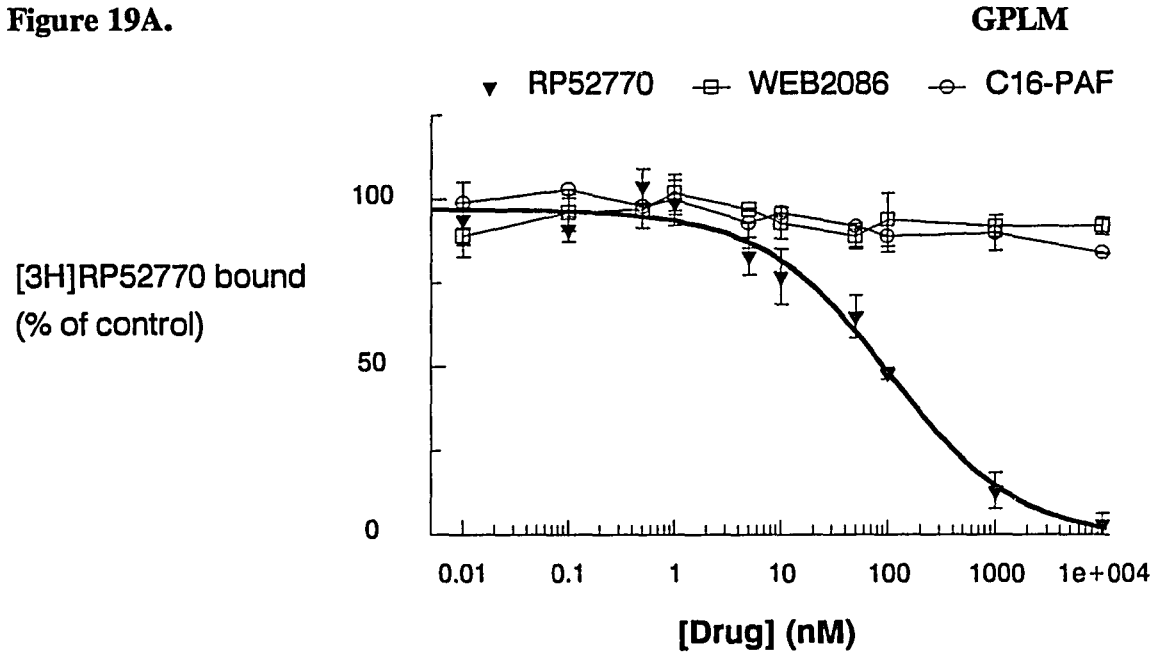

Figure 19B.

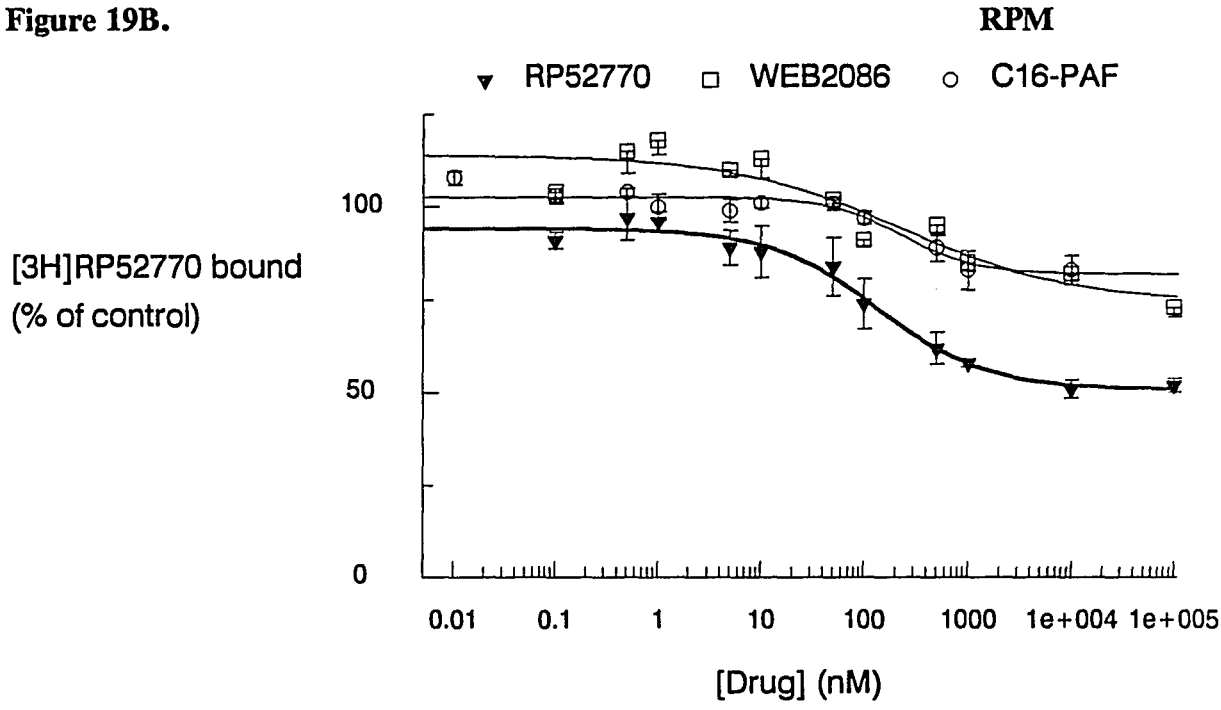

Figure 19. Inhibition of [^{3}H]RP52770 (7 nM) binding to GPLM and RPM by RP52770, WEB2086, and C_{16}-PAF. Each data point represent the mean (± SEM) of 4 experiments. Pseudo-Hill slopes and K_i values are given in the Results section.

x/÷ 2.2 for C_{16}-PAF, 84 x/÷1.6 for C_{18}-PAF, and 100 x/÷1.0 nM for WEB 2086.

Studies Examining Possible Ligand Degradation.

Saturation Experiments: These experiments were carried out with [^{3}H]C_{16}-PAF (alkyl-labeled, as used in all other experiments described above) and compared to [^{3}H]C_{16}-PAF (acetyl-labeled) in order to find out if the radioligand was being degraded by the enzyme acetylhydrolase (85). If this enzyme is present in the tissue, a difference in Bmax will be observed, i.e. the acetyl-labeled radioligand would bind less yielding a lower receptor density. Also, in parallel studies, there was no significant difference in the Bmax identified by the radioligands (*n=3*) in either tissue preparation. In GPLM, both ligands identified the same Bmax, 160 and 182 fmol/mg of protein for the radioligand alkyl-labeled and acetyl-labeled, respectively. In RPM, the Bmax values derived from these ligands were 850 and 700 fmol/mg of protein for the radioligands alkyl- and acetyl-labeled, respectively. Binding studies were performed and then free [^{3}H]C_{16}-PAF (acetyl-labeled) was collected after high speed centrifugation. No radioactivity was recovered in the supernatant after TCA precipitation (*n=3*). These results indicate that the enzyme acetylhydrolase is not

present in these tissue preparations or is not active under these conditions or temperature (4°C).

Rebinding experiments: In experiments where [^{3}H]C_{16}-PAF was recovered after incubation with tissue and was then added to fresh tissue. The results showed that specific binding was not different from the control (incubation of radioligand with fresh tissue only, *n=3*). In GPLM, specific binding of [^{3}H]C_{16}-PAF at 1 and 5 nM yielded specific binding of 50 and 120 fmol/mg protein, respectively, in control experiments. In parallel experiments, rebinding of [^{3}H]C_{16}-PAF at 1 and 5 nM yielded specific binding of 58 and 112 fmol/mg protein, respectively. In RPM, specific binding of [^{3}H]C_{16}-PAF at 1 and 5nM yielded specific binding of 450 and 1750 fmol/mg protein respectively, in control experiments. Rebinding of this radioligand at the same molar concentrations, yielded specific binding of 400 and 1800 fmol/mg protein. These results indicate that the radioligand was not being degraded and there were no soluble endogenous inhibitors present in these tissue preparations.

Receptor Digestion

Suceptibility to Heating: In both membrane preparations, there was no specific binding to [^{3}H]C_{16}-PAF (0.5 nM) after heating the tissue at 98°C for at least 15 min. (*n=3*). There was no difference between total and

nonspecific [^{3}H]C_{16}-PAF binding and the level of nonspecific binding was the same as that observed in a fresh tissue preparation.

Proteolytic Digestion: No specific binding of either [^{3}H]C_{16}-PAF (1 nM) and [^{3}H]WEB 2086 (7 nM) was observed when GPLM and RPM membranes were pre-treated with pepsin for 4 hrs at 37°C (*n*=3). Total and nonspecific binding was the same as the pattern of the nonspecific binding observed in parallel untreated tissue in the presence of 100 μM WEB 2086.

Regulation of Binding of the PAF Receptor

It has been suggested that the PAF receptor might be coupled to a guanine nucleotide regulatory protein (G protein), which can regulate cellular responses (34,37,56). Activation of a G protein in the presence of GTP promotes its uncoupling from the receptor and leads to a lower affinity state for the agonist. Experiments were carried out in the presence of GTP and analogs (nonhydrolyzable) in order to address whether the low affinity sites revealed in inhibition studies of [^{3}H]WEB 2086 by agonists are related to receptor subtypes or to a different state of the receptor upon agonist stimulation.

Effects of GTP and analogs in [^{3}H]C_{16}-PAF binding: Preliminary experiments were carried out with GTP and analogs to determine their effects on specific [^{3}H]C_{16}-PAF binding. As shown in Figure 20, specific binding of 1 nM [^{3}H]C_{16}-PAF decreased with increasing concentrations of GTP and analogs, from 0.01 to 100 μM concentration range. The GTP analog GTP-gamma-S, appeared to have the greatest effect in decreasing specific [^{3}H]C_{16}-PAF binding. The inhibition of specific [^{3}H]C_{16}-PAF binding was partial: at a concentration of 100 μM in GPLM inhibition was about 30% and in RPM about 40%. Subsequent inhibition experiments of [^{3}H]WEB 2086 by increasing concentrations of agonists were carried out in the presence of 100 μM GTP-gamma-S to test for effects on the agonist K_i values.

Effects of GTP-gamma-S and Na^+ on agonist affinity: Inhibition experiments of [^{3}H]WEB 2086 by agonist were carried out in the presence of GTP-gamma-S and Na^+. A decreased in affinity by the agonist is observed in the presence of GTP-gamma-S and Na^+. As illustrated in Figure 21A, inhibition of binding of 7 nM [^{3}H]WEB 2086 in GPLM by C_{16}-PAF in the presence of 10^{-4}M GTP-gamma-S decreased the affinity for the agonist with a K_i of 4 nM for the control and 12 nM in the presence of GTP ($p=0.05$, $n=8$). Similarly, in RPM, a decrease in affinity for the agonist from 1 nM (control) to 3 nM was observed in the presence of GTP-gamma-

Figure 20A. **GPLM**

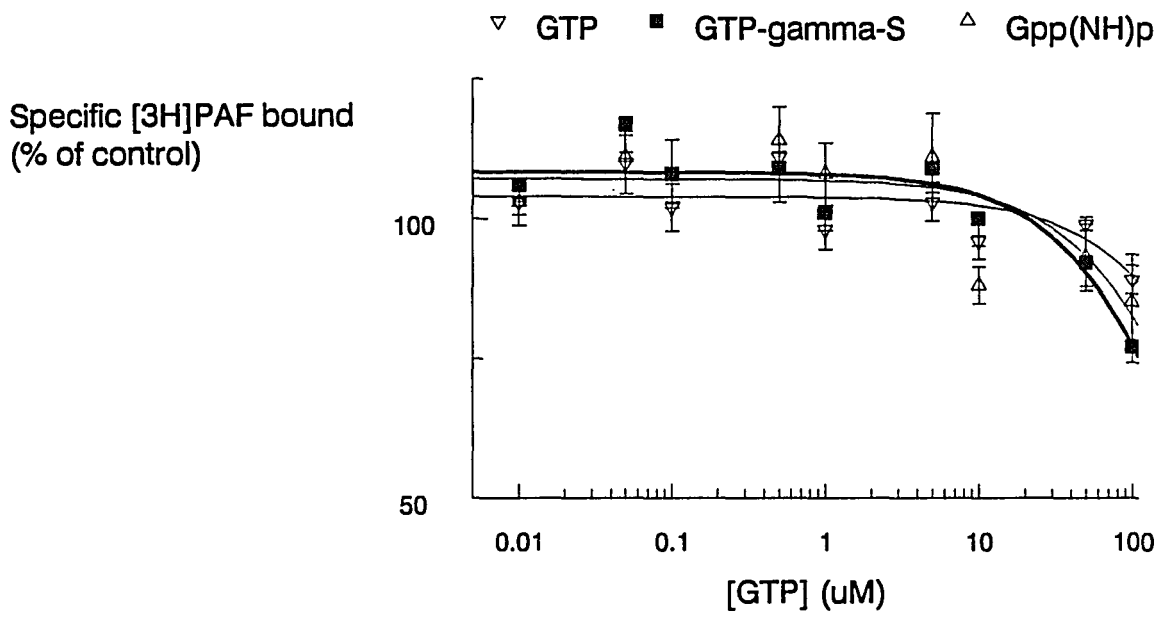

Figure 20B. **RPM**

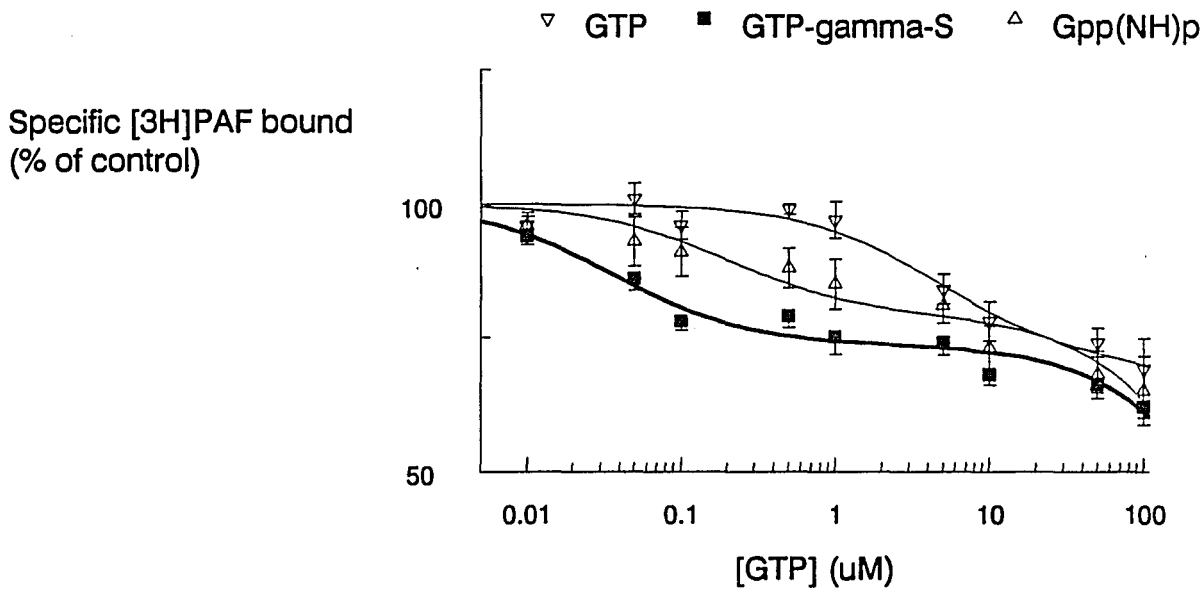

Figure 20. Effects of GTP and analogs in [^{3}H]C_{16}-PAF (1 nM) binding to GPLM and RPM. Membranes were incubated for 90 min at 25°C with 1 nM [^{3}H]C_{16}-PAF and at increasing concentrations of GTP or analogs. Each data point represent the mean (± SEM) of 4 experiments.

Figure 21A. **GPLM**

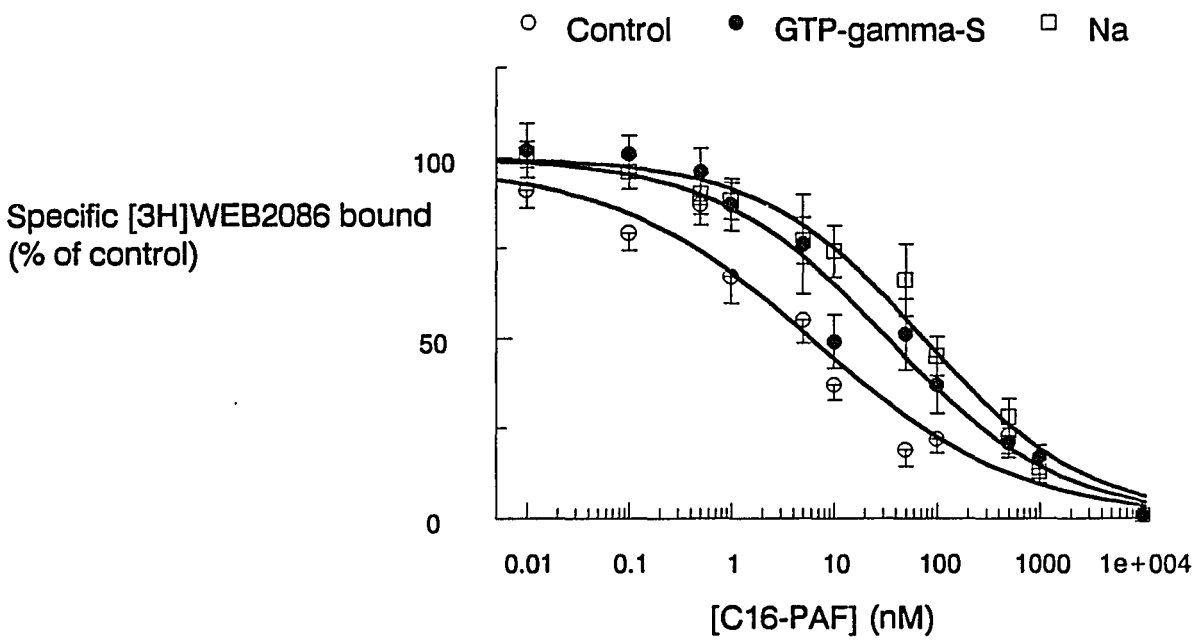

Figure 21B. **RPM**

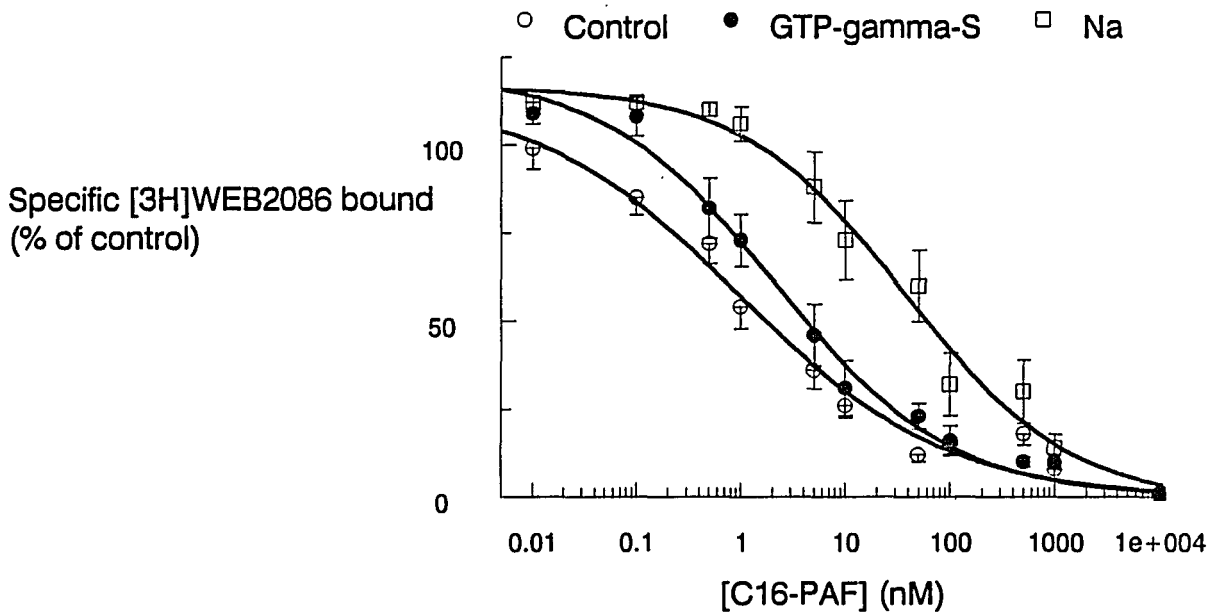

Figure 21. Inhibition of specific [^{3}H]WEB2086 (7 nM) by C_{16}-PAF in the presence of GTP-gamma-S and Na^+. Data points represent the mean (± SEM) of 8 separate experiments. Pseudo-Hill slopes and K_i values are listed in Table IV for GPLM, and Table V for RPM.

S ($p=0.002$, $n=8$). In both tissue preparations, Na^+ decreased the affinity for the agonist, from 5 to 68 nM in GPLM ($p=0.007$), and from 1 to 31 nM in RPM ($p=0.0001$). Results from inhibition data are summarized in Table IV and V. In order to determine whether GTP-gamma-S and Na^+ affected agonist but not antagonist binding, control inhibition experiments of [^{3}H]WEB 2086 binding by the unlabeled antagonist WEB 2086 were carried out in the presence of GTP-gamma-S and Na^+. As shown in Figure 22 (Table IV and V), the presence of GTP-gamma-S and Na^+ had no significant effect on the inhibition of [^{3}H]WEB 2086 (7 nM) by WEB 2086 in either GPLM or RPM ($n=4$).

Effects of pertussis and cholera toxins on agonist affinity: It has been shown that G proteins contain sites for covalent modification by pertussis and cholera toxins (25). These toxins catalyze NAD-dependent ADP-ribosylation of some G proteins, i.e. G_s and G_t serve as substrates for cholera toxin-catalyzed ADP rybosilation, and G_o and G_i serve as substrates for pertussis toxin. This covalent modification results in persistent activation of G proteins leading to uncoupling of the G protein from the receptor. In order to address whether the PAF receptor may be linked to a G protein that is pertussis or cholera toxin sensitive, membranes were treated with these toxins as described above. In both tissue preparations (shown in Figure 23 and Tables

IV and V), pertussis and cholera toxins had no effect in the affinity for C_{16}-PAF when compared to the control ($n=6$).

4. Effects of PMA on agonist binding. In addition, it has been recently shown that PMA decreases agonist binding to the PAF receptor (56) in human monocytes. However in our membrane preparation, PMA had no effect on agonist affinity (Figure 23 and Table IV and V) nor on the specific binding of [^{3}H]WEB 2086 when compared to control tissues not treated with PMA.

Figure 22A.

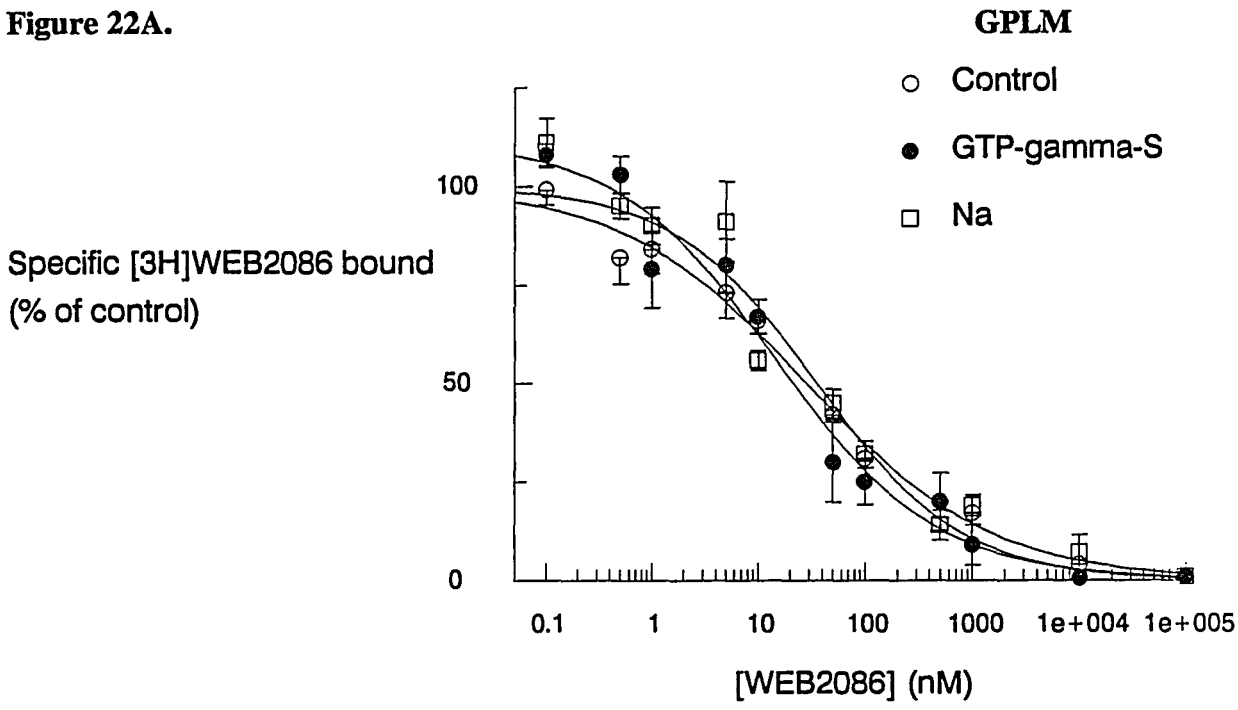

Figure 22B.

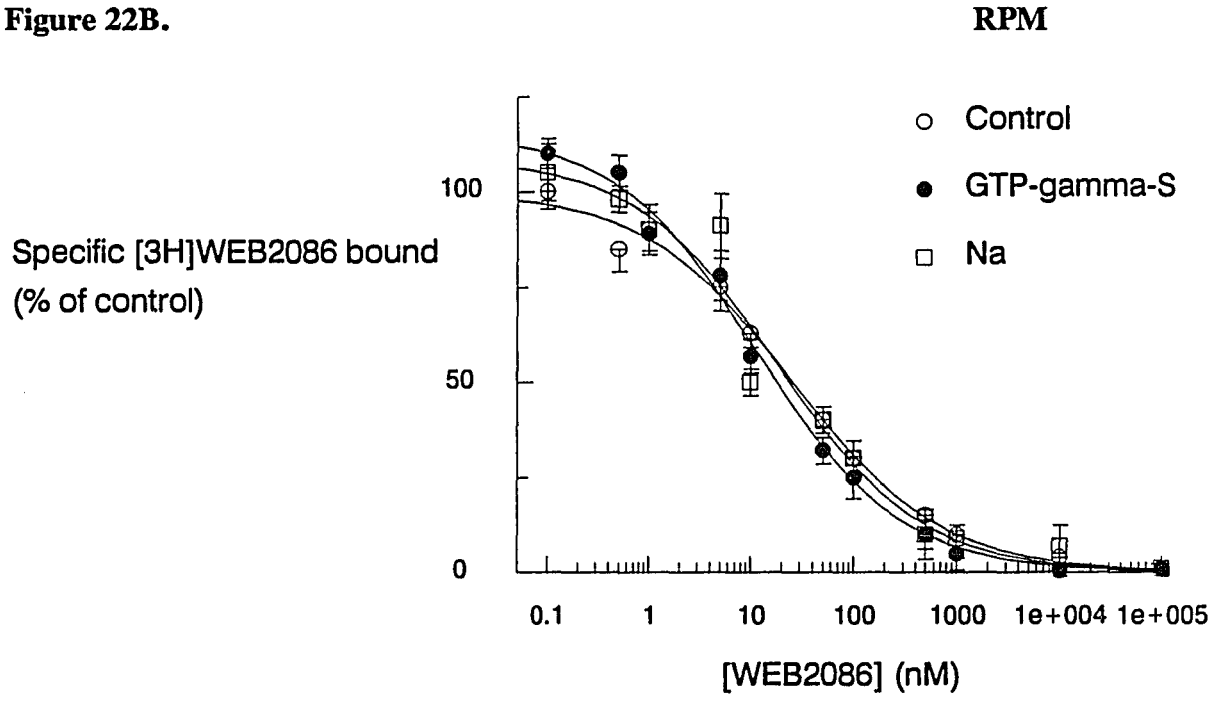

Figure 22. Inhibition of [^{3}H]WEB2086 (7 nM) by WEB2086 in the presence of GTP-gamma-S and Na^+ (n=4). Pseudo-Hill coefficients and K_i values are listed in Table IV for GPLM, and Table V for RPM.

Figure 23A.

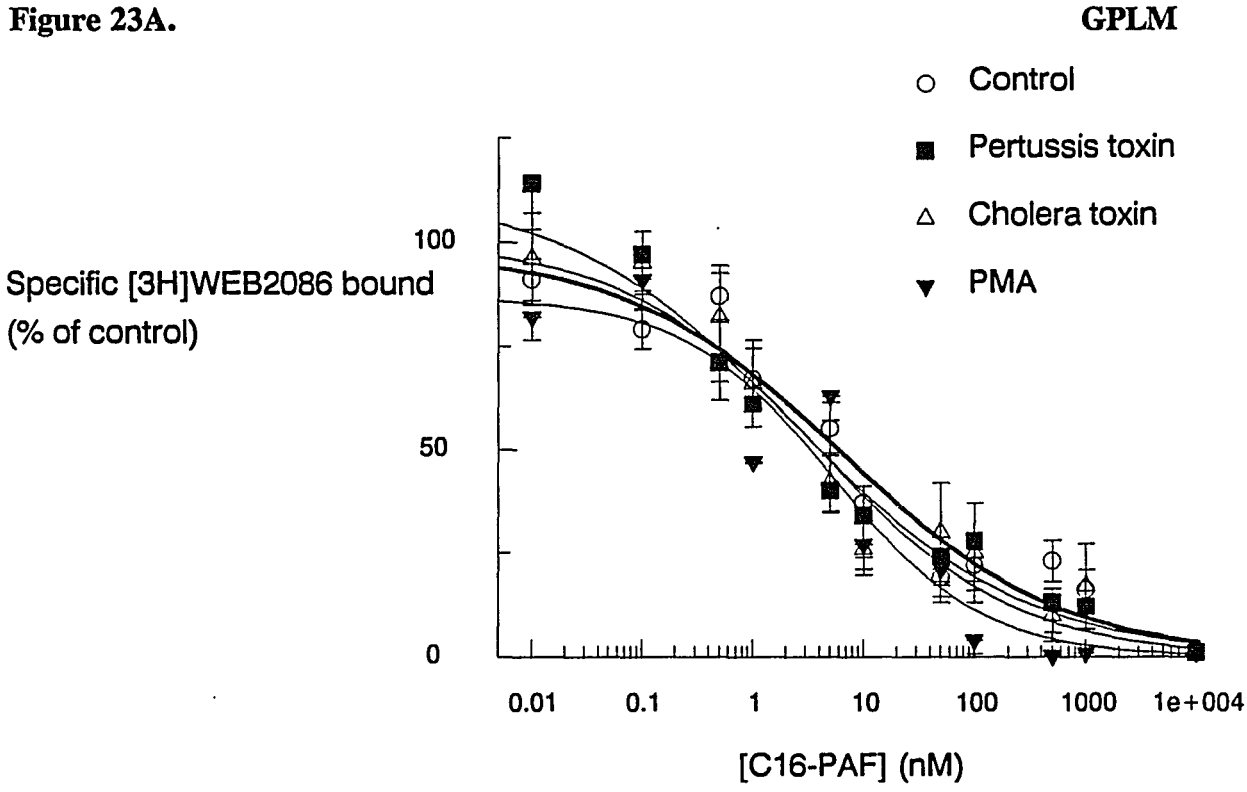

Figure 23 B.

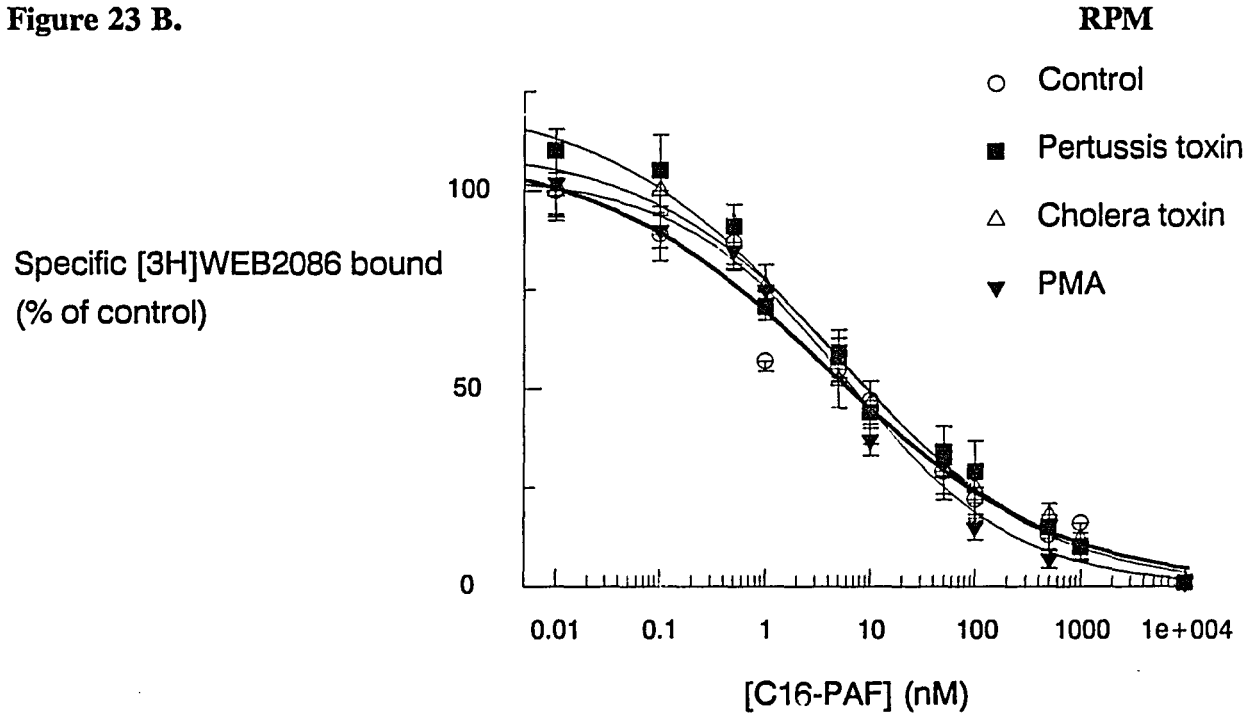

Figure 23. Inhibition of [^{3}H]WEB2086 (7 nM) binding to GPLM and RPM by C_{16}-PAF in the presence of pertussis toxin, cholera toxin or PMA. Parameters are given in Table IV for GPLM and Table V for RPM data.

TABLE IV. Inhibition of [^{3}H]WEB2086 (7 nM) binding to GPLM by C_{16}-PAF and C_{18}-PAF. Regulation of agonist binding by GTP-gamma-S, Na^+, pertussis toxin (PT), cholera toxin (CT), and PMA.

	C_{16}-PAF						C_{18}-PAF						WEB2086		
Membrane	1-site model		2-site model				1-site model		2-site model						
treatment*	K_i	n_H	K_H	$\%B_H$	K_L	n	K_i	n_H	K_H	$\%B_H$	K_L	n	K_i	n_H	n
Control	4	0.5	0.5	64	389	8	5	0.6	3	76	234	6	18	1.0	4
	(1.6)	(0.03)	(3.4)	(6)	(1.3)		(1.2)	(0.03)	(1.3)	(5)	(2.7)		(2.1)	(0.04)	
GTP	12**	0.7	3	57	372	8	24**	0.7	10	63	646	6	15	0.8	4
	(1.9)	(0.1)	(2.0)	(8)	(1.6)		(1.7)	(0.1)	(2.0)	(10)	(1.7)		(1.9)	(0.01)	
Na^+	68§	0.6	1	47	234	8	85§	0.8	4	49	676	6	17	0.8	4
	(1.6)	(0.1)	(3.9)	(5)	(1.3)		(1.2)	(0.1)	(1.2)	(13)	(2.1)		(1.2)	(0.1)	
PT	4	0.5	1	82	500	4	3	0.6				4			
	(1.2)	(0.1)	(1.3)	(9)	(2.1)		(1.9)	(0.03)							
CT	2	0.4	1	75	1015	4	4	0.7				4			
	(1.1)	(0.1)	(2.1)	(5)	(1.9)		(1.5)	(0.04)							
PMA	5	0.6	7	77	246	4	5	0.5				4			
	(1.0)	(0.04)	(1.8)	(7)	(2.2)		(1.1)	(0.1)							

* membranes were treated as described in materials and methods section. K_i values represent the geometric mean with geometric SEM in parenthesis. n_H and $\%B_H$ values represent the arithmetic mean $\pm$ SEM in parenthesis.

** K_i value significantly different from K_i value obtained from untreated tissue (C_{16}-PAF: $p=0.05$; C_{18}-PAF: $p=0.041$).

§ K_i value significantly different from K_i value obtained from untreated tissue (C_{16}-PAF: $p=0.007$; C_{18}-PAF: $p=0.0001$).

TABLE V. Inhibition of [^{3}H]WEB2086 (7 nM) binding to RPM by C_{16}-PAF and C_{18}-PAF. Regulation of agonist binding by GTP-gamma-S, Na^+, pertussis toxin (PT), cholera toxin (CT), and PMA.

	C_{16}-PAF						C_{18}-PAF						WEB2086		
Membrane	1-site model		2-site model				1-site model		2-site model						
treatment*	K_i	n_H	K_H	$\%B_H$	K_L	n	K_i	n_H	K_H	$\%B_H$	K_L	n	K_i	n_H	n
Control	1	0.6	0.4	76	214	8	4	0.5	2	64	257	4	20	1.0	4
	(1.4)	(0.1)	(2.1)	(6)	(2.7)		(2.1)	(0.04)	(1.9)	(7)	(3.0)		(1.1)	(0.03)	
GTP	3**	0.7	1	63	240	8	28**	0.6	2	47	282	4	18	0.9	4
	(1.6)	(0.1)	(1.4)	(8)	(2.1)		(1.3)	(0.1)	(2.2)	(12)	(1.9)		(1.6)	(0.04)	
Na^+	31§	0.8	8	60	309	6	20§	0.7	4	59	200	4	17	1.1	4
	(1.9)	(0.1)	(1.7)	(9)	(1.5)		(2.1)	(0.1)	(1.1)	(18)	(1.0)		(1.3)	(0.02)	
PT	2	0.6				4	4	0.6				4			
	(1.0)	(0.1)					(1.6)	(0.04)							
CT	2	0.5				4	2	0.6				4			
	(2.1)	(0.1)					(2.2)	(0.1)							
PMA	1	0.5				4	3	0.7				4			
	(2.2)	(0.1)					(1.3)	(0.1)							

* membranes were treated as described in materials and methods. K_i, n_H and $\%B_H$ values as described in Table IV.

** K_i values were significantly different from K_i values obtained from untreated tissue (C_{16}-PAF: p=0.002; C_{18}-PAF: p=0.035).

§ K_i values were significantly different from K_i values obtained from untreated tissue (C_{16}-PAF: p=0.0001; C_{18}-PAF: p=0.002).

CHAPTER IV

DISCUSSION

The pathogenesis of allergic asthma remains unclear. There is compelling evidence that bronchial asthma consists of two components: one associated with bronchospasm of the airways and the other (bronchial hyperresponsiveness) possibly associated with inflammation of the airways. Studies *in vivo* and *in vitro* have shown that in the guinea pig PAF is a mediator that mimics many of the features of asthma, including bronchial hyperresponsiveness and bronchospasm. Evidence in some cell systems, especially platelets and PMNs, indicates that PAF exerts its action(s) through a receptor-mediated mechanism and that in some cell systems there may be receptor subtypes. Therefore, in order to gain a better understanding of the role that PAF plays in bronchoconstriction in the guinea pig lung, direct radioligand binding studies were carried out in guinea pig lung membranes to determine whether specific binding sites for PAF could be demonstrated. In addition, specific binding sites for PAF in the guinea pig lung were compared to specific binding sites for PAF in rabbit platelet membranes in terms of ligand affinity, receptor density, and regulation of receptor binding.

In the studies presented herein, specific binding sites for PAF have been characterized in guinea pig lung membranes and compared to those in rabbit platelet membranes. These binding sites in GPLM and RPM were characterized with the agonist tritium-labeled C_{16}-PAF and the PAF antagonist tritium-labeled WEB 2086. Based on radioligand receptor binding studies, these binding sites are consistent with receptor sites in regard to the criteria of drug displacement, saturability, reversibility, and high affinity (44). In addition, these studies provide initial evidence for regulation of binding of the PAF receptor for agonists but not for antagonists. The binding of the PAF agonists C_{16}-PAF and C_{18}-PAF but not WEB 2086 is regulated by GTP-gamma-S and Na^+ in both guinea pig lung and rabbit platelet membranes.

Characteristics of [^{3}H]C_{16}-PAF Binding to GPLM AND RPM

In GPLM, the radioligand [^{3}H]C_{16}-PAF exhibited specific binding of relatively high affinity (K_d=3 nM) and saturability (Bmax=200 fmol/mg protein), and binding was consistent with the presence of a single type of binding sites (n_H=1.0) over the concentration range of radioligand used (0.1 to 20 nM). Similarly, in RPM, [^{3}H]C_{16}-PAF exhibited specific binding of relative high affinity (K_d=2 nM) and saturability (Bmax=3800 fmol/mg protein). The

binding was consistent with a single binding site (n_H=0.9) over the concentration range of radioligand used. Although [^{3}H]C_{16}-PAF binding in both tissue preparations yielded approximately the same affinity, in RPM the receptor density was about 20-fold greater than that estimated in GPLM. Nonspecific binding of [^{3}H]C_{16}-PAF was linear in both tissue preparations and dependent on the concentration of the radioligand. In GPLM, nonspecific [^{3}H]C_{16}-PAF binding accounted for 40% radioligand bound at 0.1 nM and 90% bound at 20 nM. In RPM, nonspecific binding of [^{3}H]C_{16}-PAF accounted for 20% of the bound at 0.1 nM and 65% at 20 nM. This difference in nonspecific binding of [^{3}H]C_{16}-PAF likely occurs because tissue concentrations are lower and receptor density is higher in RPM. Also the many different cell types in GPLM may provide additional nonspecific binding sites for [^{3}H]C_{16}-PAF compared to those measured in a single cell type, as in RPM.

Specific binding of [^{3}H]C_{16}-PAF reached steady-state by 6 hrs in GPLM and by 4 hrs in RPM (Figure 8). Characteristically, nonspecific binding of [^{3}H]C_{16}-PAF reached equilibrium (plateau levels) very quickly and did not change thereafter. An important feature of ligand-receptor interactions is that the specific binding should be reversible (44,87), and this is clearly shown in kinetic studies (Figure 9) whereby dissociation of [^{3}H]C_{16}-PAF was

initiated after steady-state binding was achieved. Importantly in this regard, the K_d values derived from kinetic and saturation isotherm studies are in agreement with each other. Some previous reports have indicated that in intact cells the binding of [^{3}H]C_{16}-PAF is only partially reversible (33,42,58,84,). These observations imply that [^{3}H]C_{16}-PAF may have been taken up (by a non receptor mechanism) into the membrane or cytosolic phase of the cell, or the receptor-ligand complex may have been internalized and becoming inaccessible to unlabeled antagonists. In the studies described here, the use of a membrane preparation (rather than whole cells) may account for these differences in degree of reversibility of binding, a possibility supported by data from studies using plasma membrane from other cell types (39,40).

In general, binding characteristics of the PAF receptor have been shown to vary in different cells types, and even for the same cell type; i.e. K_d values for [^{3}H]PAF binding to human platelets vary from 0.01 to 30 nM (40,42,81,83,84). In addition, receptor densities for human platelets have also been shown to vary from 270 to 1400 sites/cell (42,84) a 5-fold difference in receptor density. Similarly, discrepancies regarding receptor densities in rabbit platelets have also been reported; i.e. from 400 to 2400 sites/cell (33,70). These variations (regarding K_d and

Bmax) were most likely related to different experimental conditions or to different PAF receptors. Thus there was a need for studies performed under identical conditions such as those described here to address the issue of whether there is more than one receptor type for [^{3}H]C_{16}-PAF in different cells and tissues. Although the studies described here revealed different receptor densities, K_d values were similar in GPLM and RPM and thus were not supportive of different receptor types.

Specific binding of [^{3}H]C_{16}-PAF to GPLM and RPM was inhibited in a dose dependent manner by C_{16}-PAF, C_{18}-PAF, and the PAF antagonists WEB 2086 and RP52770. The inactive PAF metabolite lyso-C_{16}-PAF failed to inhibit the specific binding of [^{3}H]C_{16}-PAF. In these studies, the K_i value from inhibition data for C_{16}-PAF (7 nM) was not significantly different from the K_d value derived from saturation studies (3 nM) in GPLM. Similarly, in RPM the K_i value derived from inhibition data (1.0 nM) was not significantly different from that derived from direct saturation studies (1 nM). In addition, binding of [^{3}H]C_{16}-PAF (0.5 nM) was inhibited to the same extent by (unlabeled) C_{16}-PAF, C_{18}-PAF, WEB 2086 and RP52770 in both GPLM and RPM (Figure 12, and Tables II, III). These observations suggest that C_{16}-PAF, C_{18}-PAF, WEB 2086 and RP52770 inhibit [^{3}H]C_{16}-PAF binding, likely by interacting at the same binding site.

In these studies, binding experiments were best carried out in 50 mM Tris buffer (pH 7.2) containing 5 mM $MgCl_2$ and 2.5 mg/ml BSA. Since PAF is a phospholipid, BSA was needed to provide solubility in an aqueous solution. Although PAF requires the presence of BSA (43) high concentrations of BSA have been shown to inhibit biologic activity of PAF (33). Previous radioligand binding studies have used a range of BSA concentrations from 0.25 to 2.5 mg/ml (39,40,48,58,70,82). It has been demonstrated herein that BSA affects both specific and nonspecific binding (Figure 3). Although a BSA concentration of 2.5 mg/ml was selected as optimal, this condition might vary in other tissue preparations or with different binding conditions and should be examined separately for other preparations. Because of the complexity that BSA adds to the interactions of $[^3H]C_{16}$-PAF with its receptor, the K_d values should be regarded as approximate. These studies point to a need for future studies designed to establish the nature of the PAF-BSA interaction, if the PAF solubility issue can be solved.

Characteristics of $[^3H]$WEB 2086 Binding to GPLM AND RPM

In the course of the studies described here, several problems associated with using $[^3H]C_{16}$-PAF as ligand were revealed: (a) as described above, PAF needs a carrier protein for solubility, (b) PAF shows high nonspecific

binding capacity especially in GPLM, and (c) PAF may induce receptor conformational changes when binding to its receptor site since it is an agonist. Because of (c), antagonists rather than agonists are preferred ligands for binding, particularly when the antagonist belongs to a different chemical class (44,87). Thus, tritium-labeled WEB 2086 (a PAF antagonist) was also used to label the PAF binding site in GPLM and RPM.

Specific binding of [^{3}H]WEB 2086 to GPLM and RPM reached steady-state by 4 and 3 hrs, respectively (Figure 13). Characteristically, nonspecific binding of [^{3}H]WEB 2086 reached plateau levels before the specific binding with no changes thereafter. Reversibility of [^{3}H]WEB 2086 binding was shown in dissociation experiments and was initiated after steady-state binding was achieved (Figure 14). Importantly, this ligand does not require a carrier protein since it is soluble in an aqueous media. Also, it is an antagonist chemically different from PAF (Figure 2).

In GPLM, the binding of [^{3}H]WEB 2086 was of relative high affinity (K_d=42 nM), was saturable (Bmax=226 fmol/mg protein), and was displaceable by C_{16}-PAF, C_{18}-PAF (Figure 16), WEB 2086, and RP52770 (Figure 17), but not by lyso-C_{16}-PAF. In both tissue preparations, receptor densities identified by [^{3}H]WEB 2086 were not significantly different from those identified by [^{3}H]C_{16}-PAF (Table I).

Inhibition of [^{3}H]WEB 2086 (7 nM) binding by agonists (but not by antagonists) yielded shallow inhibition curves, in both tissue preparations (Figure 16) and yielded pseudo-Hill coefficients significantly less than unity (Tables II, III). These shallow inhibition curves by agonists are consistent with either multiple conformational states or different receptor subtypes (44,87).

From these studies we concluded therefore, that [^{3}H]WEB 2086 is a suitable PAF antagonist in guinea pig lung and rabbit platelet membrane preparations, because: a) [^{3}H]WEB 2086 shows low nonspecific binding, b) [^{3}H]WEB 2086 binds to the same receptor density as [^{3}H]C_{16}-PAF, and c) the potencies of inhibition by unlabeled agonists and antagonists in [^{3}H]WEB 2086 are the same as those observed in [^{3}H]C_{16}-PAF. These data provide evidence that the ability of PAF to induce and WEB 2086 to antagonize, at least some of the functional effects of PAF <u>in vivo</u> and <u>in vitro</u> in guinea pig (67,57) and rat (13), occur by direct receptor interactions.

Evidence for Regulation of Binding of PAF AND Receptor Heterogeneity

Radioligand binding studies commonly reveal inhibition curves which are shallow when unlabeled agonist is employed to inhibit binding of radiolabeled antagonist. Shallow

inhibition curves arise from a) cooperativity (binding of one molecule of ligand affecting the binding of another molecule at a nearly site), b) the existence of receptor subtypes with different binding affinities, or c) the existence of different receptor states depending on conformational changes which occur as a result of interactions of the receptor with cytoplasmic or membrane associated proteins. One way of determining whether the latter of these three is responsible for shallow inhibition curves is to demonstrate that affinity is reduced and that inhibition curves become steeper in the presence of substances known to uncouple the receptor from association with regulatory proteins, i.e. G proteins.

Like the data presented here, recent studies of the PAF binding in rabbit platelet membranes yielded shallow inhibition curves for C_{16}-PAF and C_{18}-PAF, with pseudo-Hill coefficients less than unity (36). These investigators went on to suggest that in RPM, the PAF receptor might be coupled to a G protein since a decrease in affinity for the agonists was observed (shift to the right) when GTP was included in the incubation media. In the studies presented herein, GTP-gamma-S significantly decreased the affinity for C_{16}-PAF, from 4 nM (control) to 12 nM (in the presence of 100 μM GTP-gamma-S) in GPLM ($p=0.05$), and from 1 nM to 3 nM in RPM ($p=0.002$). Similarly, in GPLM GTP-gamma-S significantly

decreased the affinity for C_{18}-PAF from 5 nM to 24 nM p=0.04 (Table IV). Also in RPM a decrease in affinity was observed for C_{18}-PAF, from 4 to 28 nM (p=0.035) when GTP-gamma-S was included in the incubation media.

The observations with and without the GTP analog suggest that, in both tissue preparations, the PAF receptor exists in more than one affinity state or site for the agonist. Some portion of the PAF receptor population appears to be coupled to a G protein since presence of a GTP analog has a small effect on the affinity state for agonist. The G protein is susceptible to activation by GTP-gamma-S, leading to a decrease in affinity for agonists (small rightward shift). These observations are in agreement with those by others (1,15,62), who have studied other receptor-ligand systems and have shown that G proteins can be persistently activated by nonhydrolyzable GTP analogs. As a result, the G proteins are uncoupled from the receptor, leading to a lower affinity state for agonists but not antagonists. It is important to point out that in both tissue preparations the inhibition curves in the presence of GTP-gamma-S were still shallow, yielding pseudo-Hill coefficients that were somewhat greater than the control but were significantly less than unity (for both GPLM and RPM n_H= 0.7; Tables IV, V). Similarly, the inhibition curves of C_{18}-PAF in the presence of GTP-gamma-S were shallow and

yielded pseudo-Hill coefficients significantly less than unity (GPLM=0.7, RPM=0.6). In addition, the K_H, the K_L and the $\%B_H$ were not significantly different from those values obtained from the control (untreated tissue) for C_{16}-PAF and C_{18}-PAF in both tissue preparations (see Tables IV, V). These observations suggest that the PAF binding site remains heterogeneous in nature even after GTP-gamma-S treatment and suggest that K_H and K_L populations of PAF binding sites remain different in the presence of GTP-gamma-S. Therefore, it is possible that there is more than one subtype of receptor within the population of high affinity sites, and that one subtype is GTP sensitive (coupled to G protein), and the other is not. Further studies in GPLM and RPM will determine whether this agonist-associated heterogeneity in binding sites is related to receptor subtypes.

Contrary to the effects of GTP-gamma-S in agonist binding, no effects on the affinity of WEB 2086 were observed when membranes were treated with GTP-gamma-S (Tables IV, V) in either tissue preparation. These observations are in accord with the possibility that GTP-gamma-S affects the receptor by decreasing the affinity for agonist binding but not for antagonist binding.

Subsequent studies were directed toward characterizing further the regulation of agonist binding to the PAF receptor in GPLM and RPM. The esperimental design was based

on previous studies establishing that some G proteins are susceptible to being irreversibly activated by pertussis toxin and cholera toxin (1,25). In both, GPLM and RPM, the affinity of the receptors for agonists was not affected by pertussis and cholera toxin treatment (Tables IV, V). These results indicate that in GPLM and RPM, the putative G protein involved in regulating agonist binding (GTP-gamma-S activated) is not a substrate for pertussis or cholera toxin. Studies by others have shown that some G proteins are GTP-dependent, but insensitive to cholera or pertussis toxin (34,24). In human platelets, PAF has been shown to stimulate GTPase activity in a dose dependent manner (34). The activation of GTPase led to phosphatidylinositol metabolism that was cholera and pertussis toxin-insensitive. This suggests the involvement of a G protein different from those previously characterized as cholera sensitive (G_s, G_t) or pertussis sensitive (G_o, G_i, G_t). Contrary to these observations, activation of rabbit neutrophils by PAF leads to phosphatidylinositol metabolism and neutrophil degranulation (56), events that were abolished by pretreatment of cells with pertussis toxin. However, activation of rabbit neutrophils also leads to intracellular Ca^{++} mobilization through pertussis toxin-insensitive events. These studies suggest that there might be more than one receptor subtype in rabbit neutrophils: one that induces

Ca^{++} mobilization (pertussis-insensitive) at PAF concentrations between $1x10^{-11}$ and $1x10^{-8}$ M; and the other linked to the phosphatidylinositol metabolism (pertussis-sensitive) at PAF concentrations between $1x10^{-8}$ to $5x10^{-7}$ M, which results in cell degranulation. The data obtained here are consistent with the possibility that in the GPLM and RPM, there might be more than one receptor subtype: one sensitive to GTP-gamma-S, and probably two (one high and low affinity) insensitive to GTP-gamma-S. In any case, these receptor subtypes are not coupled to G proteins sensitive to cholera or pertussis toxins.

Several studies have indicated the requirement of Na^+ (in addition to GTP) for activation of G_i which in turn leads to inhibition of adenylate cyclase. This is the case with muscarinic cholinergic receptors (1), and opioid receptors (62). In the present studies, treatment of membranes with Na^+ affected the affinity for agonists but not for antagonists (Tables IV, V). In GPLM, the presence of Na^+ significantly decreased the affinity for C_{16}-PAF from 4 to 68 nM ($p=0.007$; Table IV, Figure 21A) and the affinity of C_{18}-PAF from 5 to 85 nM ($p=0.0001$; Table IV). Similarly, in RPM, Na^+ decreased the affinity for C_{16}-PAF from 1 to 31 nM ($p=0.0001$ Table V, Figure 21B), and for C_{18}-PAF, from 4 to 20 nM ($p=0.002$; Table V). In these studies, the K_H or K_L for the two-site fit or the $\%B_H$ were not significantly

different from those values obtained from the control. As previously addressed for the GTP-sensitive studies, there is a possibility of more than receptor subtype within the population of high affinity sites, and that one subtype is GTP sensitive and the other Na^+ sensitive. However, the possibility that GTP-gamma-S and Na^+ have the same effects on a putative G protein should also be considered. Previous studies in the opioid receptors indicated that in all three subtypes of receptors the presence of Na^+ plus Gpp(NH)p (a GTP analog) largely decreased the binding affinity for their respective agonist (62), possibly by uncoupling the G protein, which in turn led to inhibition of the adenylate cyclase activity. In recent studies in rabbit platelet membranes, it was shown that the combination of GTP plus Na^+ decreased the binding affinity for C_{16}-PAF (from 1 nM to 2.3 μM) and yielded steep inhibition curves with pseudo-Hill coefficients of unity. These latter observations, as those in the present studies, suggest that GTP and analogs decrease the receptor affinity for C_{16}-PAF. Therefore, the receptors might not be in a single conformational state but may be rather in multiple conformational states. Further studies in GPLM and RPM will be required in order to determine whether this agonist-associated heterogeneity in binding in the presence of GTP-gamma-S and/or Na^+ occurs

because of interrelated sites or whether separate entities or receptor subtypes are present.

Radioligand Binding Studies with [^{3}H]RP52770

During the course of these studies, a report of a new PAF antagonist (RP52770) was published (70). Because it appeared to be more potent than WEB 2086, characterization of its binding capacity in GPLM and RPM was examined. Unlabeled RP52770 was first shown to be capable of inhibiting [^{3}H]C_{16}-PAF binding in GPLM and RPM with K_is of 7 and 2 nM, respectively. However, in GPLM, unlabeled C_{16}-PAF, C_{18}-PAF, and WEB 2086 failed to inhibit the binding of the PAF antagonist [^{3}H]RP52770. Only unlabeled RP52770 inhibited the binding of this ligand and yielded a K_i of 35 nM and pseudo-Hill coefficients of unity (Figure 19A). In addition, saturation experiments with [^{3}H]RP52770 indicated that this radioligand identifies a receptor population of much higher density (Bmax of 1620 fmol/mg of protein, Table I) than that identified by [^{3}H]C_{16}-PAF (Bmax=200 fmol/mg p) and [^{3}H]WEB 2086 (Bmax=226 fmol/mg p). These results are similar to those observed by others in human platelets (82), where [^{3}H]RP52770 was found to identify a receptor density 7-fold higher than those identified by [^{3}H]PAF and [^{3}H]WEB 2086. The results presented indicate that, in GPLM, [^{3}H]RP52770 binds to a site in addition to the PAF binding

site. Importantly, in this tissue preparation the [^{3}H]RP52770 binding sites appear to be a combination of sites of which only a small percentage represent the PAF binding sites.

In RPM, unlabeled RP52770 inhibited 50% of the total [^{3}H]RP52770 bound and unlabeled C_{16}-PAF, C_{18}-PAF, and WEB 2086 inhibited 50% of the specific binding (Figure 19B). Saturation experiments with [^{3}H]RP52770 in RPM indicate that this radioligand identifies a receptor population of much higher density with a Bmax of 10105 fmol/mg of protein than that identified by [^{3}H]C_{16}-PAF (Bmax=1922 fmol/mg p) and [^{3}H]WEB 2086 (Bmax=2639 fmol/mg p). The present results are in contention with those studies in intact rabbit platelets where the receptor density identified by [^{3}H]RP52770 was the same as that by [^{3}H]PAF (48,70). The difference between these findings and those in the present study may be due to different binding conditions and the use of whole cells rather than membrane preparations.

Therefore, it appears that in GPLM the [^{3}H]RP52770 binding sites are present with a much greater receptor density (8-fold difference) than the [^{3}H]C_{16}-PAF binding sites. In addition, the [^{3}H]RP52770 binding site can not be inhibited by unlabeled C_{16}-PAF, C_{18}-PAF, or WEB 2086. In RPM, the [^{3}H]RP52770 binding sites are also present at a greater density (4-fold greater density) than the [^{3}H]C_{16}-

PAF. However, this difference, is less than that in GPLM. Thus the PAF sites may represent a larger population of the total RP52770 binding sites in RPM and therefore, binding is detectably (but only partially) inhibited.

CHAPTER V

CONCLUSIONS

The present results support evidence that these PAF binding sites are in effect receptor sites. The data further establishes that these binding sites are consistent with receptor sites. The data also provide an initial characterization with respect to of transducing mechanisms and regulation of the PAF receptor.

The present studies also present evidence that some of the PAF receptors in GPLM and RPM are coupled to a putative G protein, which can be activated by GTP-gamma-S. This putative G protein is not cholera or pertussis toxin sensitive. In addition, these studies provide evidence that Na^+ may play a role in regulating binding of PAF species by a still undefined mechanism. Evidence presented suggest that there appears to be more than one agonist affinity state for C_{16}-PAF, and C_{18}-PAF in both GPLM and RPM, and possibly more than one receptor subtype. Radioligand binding studies in GPLM and RPM suggest that C_{16}-PAF C_{18}-PAF, and WEB 2086 bind to the same receptor site. The PAF antagonist RP52770 binds to a PAF site an additional site. This other RP52770 binding site appears to represent the majority of the RP52770 sites and does not bind to the PAF species studied: C_{16}-PAF and C_{18}-PAF or to WEB 2086. It is

not known whether these other RP52770 binding sites will interact with other PAF homologs and/or analogs.

The presence of specific binding sites for PAF in guinea pig lung membranes represent an initial step in determining whether the PAF-induced contraction of peripheral lung strips occurs by activation of these receptors. Although these studies were carried out in peripheral lung membranes and did not localize the specific cell type(s) that bear the PAF receptor, it is important to emphasize that this tissue shows high affinity for [^{3}H]C_{16}-PAF and [^{3}H]WEB 2086. Rabbit platelet membranes also showed high affinity for both radioligands, and these findings are in accord with those reported by others in terms of K_d for [^{3}H]C_{16}-PAF (33,40,70), and receptor density.

Identifying the PAF receptor distribution in GPLM might help to develop the link between binding and biological activity. In some species, including the guinea pig, PAF has been shown to mediate bronchoconstriction (46,57,71). These studies have shown that the PAF antagonist BN 52021 markedly reduced bronchoconstriction caused by aerosolized antigen. Similar studies have shown that WEB 2086 partially abolished the contraction of guinea pig isolated lung strips when challenged by antigen (67). Moreover, <u>in vivo</u> pretreatment with WEB 2086 abolishes the bronchoconstriction evoked by i.v. infusion of PAF and partially inhibited

bronchoconstriction induced by antigen in passively sensitized guinea pigs. These studies imply that WEB 2086 antagonizes the *in vivo* bronchoconstrictive effects evoked by i.v. infusion of PAF or antigen (57,67).

The demonstration of specific binding sites for [^{3}H]C_{16}-PAF and [^{3}H]WEB 2086 in GPLM does not prove that contraction induced by PAF in human and guinea pig lungs is directly mediated by PAF receptors; however it is consistent with this possibility. Identification of the lung cell types that have the PAF binding sites will require further studies. The characterization of [^{3}H]WEB 2086 as a specific antagonist of the PAF binding site in GPLM and RPM will facilitate this task. Further studies involving receptor localization (in GPLM) to specific cell types are needed since there is no assurance that observed binding sites are relevant to lung contraction, rather than to some other lung response. A through understanding of the localization and function of lung PAF receptors will provide a basis for establishing the mechanisms by which this potent autacoid participates in normal and/or abnormal lung function.

LIST OF REFERENCES

1. Ashkenazi, A; Winslow, JW; Peralta, EG; Peterson, GL; Schimerlik, MI; Capon, DJ; and Ramachandran, J. An M_2 muscarinic receptor subtype coupled to both adenylyl cyclase and phosphoinositide turnover. Science; 1987; 238: 672-675.

2. Bachelet, M.; Masliah, J.; Vargaftig, B.B.; Bereziat, G.; and Colard, O. Changes induced by PAF-acether in diacyl and ether phospholipids from guinea-pig alveolar macrophages. Biochimica Biophysica Acta; 1986; 878: 177-183.

3. Barbaro, J.F.; and Zvaifler, Nathan J. Antigen induced histamine release from platelets of rabbits producing homologous PCA antibody. Proc Soc Exp Biol Med; 1966; 120: 1245-1247.

4. Barnes, Peter J. Platelet-activating factor and asthma. J. of Allergy and Clinical Immunology; 1989; 81(1): 152-160.

5. Barnes, PJ; Chung, KF; and Page, CP. Inflammatory mediators and asthma. Pharmacol Rev; 1988; 40: 49-84.

6. Benveniste, J; Le Couedic, JP; Polonsky, J; and Tence, M. Structural analysis of purified platelet-activating factor by lipases. Nature; 1977; 269: 170-171.

7. Benveniste, J.; Henson, P.M.; and Cochrane, C.G. Leukocyte-dependent histamine release from rabbit platelets. The role of IgE, basophils and a platelet activating factor. J Exp Med; 1972; 136: 1356-1377.

8. Braquet, P; Touqui, L; Shen, TY; and Vargaftig, BB. Perspectives in Platelet-activating factor research. Pharmacol Rev; 1987; 39: 97-145.

9. Brock, T.A.; and Gimbrone, M.A. Platelet activating factor alters calcium homeostasis in cultured vascular endothelial cells. American Journal of Physiology; 1986; 252: H1086-H1092.

10. Bruynzeel P.L.B.; Koenderman L.; Kok P.T.M.; Hameling M.L.; and Verhagen J. Platelet-Activating Factor (PAF-Acether) induced Leukotriene C4 formation and luminol dependent chemiluminescence by human eosinophils. Pharmacological Research Communications; 1986; 18(Suppl.): 61-69.

11. Bussolino, F; Agglietta, M; Sanavio, F; Stacchini, A; Lauri, D; Camussi, G. Alkyl-ether phosphoglycerides influence calcium fluxes into human endothelial cells. The Journal of Immunology; 1985; 135(4): 2748-2753.

12. Camussi, G; Bussolino, F; Tetta, C; Piacibello, W; and Aglietta, M. Biosynthesis and release of platelet-activating factor from human monocytes. Int Arch Allergy Appl Immunol; 1983; 70: 245-251.

13. Casals-Stenzel, J; Franke, J; Friedrich, T; and Lichey, J. Bronchial and vascular effects of PAF in the rat isolated lung are completely blocked by WEB 2086, a novel specific PAF antagonist. Br. J. Pharmacol.; 1987; 91: 799-802.

14. Casals-Stenzel, Jorge. Effects of WEB 2086, a novel antagonist of platelet activating factor, in active and passive anaphylaxis. Immunopharmacology; 1987; 13: 117-124.

15. Catanese, CA; Falcone, RC; and Aharony, D. Guanyl-5'-ylimidodiphosphate regulation of ligand binding to LTD_4 receptors on guinea pig lung membranes. J Pharmacol Exp Ther; 1989; 251: 846-851.

16. Cheng, Y.C.; and Prusoff, W.H. Relationship between the inhibition constant (K_i) and the concentration of inhibitor which causes 50 percent inhibition (IC_{50}) of an enzymatic reaction. Biochemical Pharmacology; 1973; 22: 3099-3108.

17. Chignard, M; Le Couedic, JP; Tence, M; Vargaftig, BB; and Benveniste, J. The role of platelet-activating factor in platelet aggregation. Nature; 1979; 275: 799-800.

18. Cirino, M.; Lagente, V.; Lefort, J.; and Vargaftig, B.B. A study with BN 52021 demonstrates the involvement of PAF-acether in IgE-dependent bronchoconstriction. Prostaglandins; 1986; 32(1): 121-126.

19. Cuss, FM; Dixon, CMS; and Barnes, PJ. Effects of inhaled platelet activating factor on pulmonary function and bronchial responsiveness in man. Lancet; 1986: 189-192.

20. De Monchy, J.G.R.; Kauffman, H.F.; Venge, P.; Koeter, G.H.; Jansen, H.M.; Sluiter, H.J.; and de Vries, K. Bronchoalveolar eosinophilia during allergen-induced late asthmatic reactions. Am Rev of Resp Dis; 1985; 131: 373-376.

21. DeLean, A.; Hancock, A.A.; and Lefkowitz, R.J. Validation and statistical analysis of a computer modeling method for quantitative anlysis of radioligand binding data for mixtures of pharmacological receptor subtypes. Mol Pharmacol; 1982; 21: 5-16.

22. Demopolous, Constantinos A.; Pinckard, Neal R.; Hanahan, Donald J. Platelet-Activating Factor. Evidence for 1-O-alkyl-2-acetyl-sn-glyceryl-3-phosphorylcholine as the active component (a new class of lipid chemical mediators). J Biol Chem; October 10, 1979; 254(19): 9355-9358.

23. Feldman, HA. Mathematical theory of complex ligand-binding systems at equilibrium. Anal Biochem; 1972; 48: 317-338.

24. Fong, HK; Yoshimoto, KK; Eversole-Cire, P; and Simon, MI. Identification of a GTP-binding protein alpha subunit that lacks an apparent ADP-ribosylation site for pertussis toxin. Proc Natl Acad Sci USA; 1988; 85: 3066-3070.

25. Freissnuth, Michael; Casey, Patrick J.; and Gilman, Alfred G. G proteins control diverse pathways of transmembrane signaling. FASEB J; 1989; 3: 2125-2131.

26. Goetzl, EJ; Derian, CK; Tauber, AI; and Valone, FH. Novel effects of 1-O-hexadecyl-2-acyl-*sn*-glycero-3-phosphocholine mediators on human leukocyte function: Delineation of the specific roles of acyl substituents. Biochem Biophys Res Commun; 1980; 94: 881-888.

27. Hanahan, D.J.; Demopoulos, C.A.; Liehr, J. and Pinckard, R.N. Identification of platelet-activating factor isolated from rabbit basophils as acetyl glyceryl ether phosphorylcholine. J Biol Chem; 1980; 255: 5514-5516.

28. Hartung, Hans-Peter. Acetyl glyceryl ether phosphorylcholine (platelet-activating factor) mediates heightened metabolic activity in macrophages. Studies on PGE, TXB2 and O_2 production, spreading, and the influence of calmodulin-inhibitor W-7. FEBS; 1983; 160(1,2): 209-212.

29. Hartung, Hnas-Peter; Parnham, Michael J.; Winkelmann, Johannes; Englberger, Werner; Hadding, Ulrich. Platelet activating factor (PAF) induces the oxidative burst in macrophages. Int J of Immunopharmacology; 1983; 5(2): 115-121.

30. Hayashi, H; Kudo, I; Inoue, K; Onozaki, K; Tsushima, S; Nomura, H; Nojima, S. Activation of guinea pig peritoneal macrophages by platelet activating factor (PAF) and its agonists. J Biochem; 1985; 97(6): 1737-1745.

31. Henson, Peter M. Mechanisms of release of constituents from rabbit platelets by antigen-antibody complexes and complement. I. Lytic and nonlytic reactions. Immunology; 1969; 105(2): 476-489.

32. Hill, AW. The possible effects of the aggregation of the molecules of hemoglobin on its dissociation curves. J Physiol; 1910; 40: iv-vii.

33. Homma, H; Tokumura, A; Hanahan, DJ. Binding and internalization of platelet-activating factor 1-O-alkyl -2-acetyl-sn-glycero-3-phosphocholine in washed rabbit platelets. J Biol Chem; 1987; 262(22): 10582-10587.

34. Houslay, MD; Bojanic, D; and Wilson, A. Platelet activating factor and U44069 stimulate GTPase activity in human platelets which is distinct from the guanine nucleotide regulatory proteins, N_s and N_i. Biochem J.; 1986; 234: 737-740.

35. Humphrey, DM; McManus, LM; Satouchi, K; Hanahan, DJ; and Pinckard, RN. Vasoactive properties of acetyl glyceryl ether phosphorylcholine (AGEPC) and AGEPC analogues. Lab Invest; 1982; 46: 422-427.

36. Hwang, S-B.; Lam, M-H.; and Hsu, A. H-M. Characterization of platelet-activating factor (PAF) receptor by specific binding of [^{3}H]L-659,989, a PAF receptor antagonist, to rabbit platelet membranes: possible multiple conformational states of a single type of PAF receptors. Mol Pharmacol; 1989; 35: 48-58.

37. Hwang, San-Bao; Lam, My-Hanh; and Pong, Sheng-Shung. Ionic and GTP regulation of binding of platelet-activating factor to receptors and platelet-activating factor-induced activation of GTPase in rabbit platelet membranes. J Biol Chem; 1986; 261(2): 532-537.

38. Hwang, San-Bao; Lam, My-Hanh; Shen, T.Y. Specific binding sites for platelet activating factor in human lung tissue. Biochemical and Biophys Res Commun; 1985; 128(2): 972-979.

39. Hwang, S-B; Lam, M-H; Shen, T.Y. Specific binding sites for platelet activating factor in human lung tissue. Biochem Biophys Res Commun; 1985; 128(2): 972-979.

40. Hwang, S-B; Lee, C-S C.; Cheah, M J; Shen, T.Y. Specific receptor sites for 1-O-alkyl-2-O- acetyl-sn-glycero-3-phosphocholine (Platelet activating factor) on rabbit platelet and guinea pig smooth muscle membranes. Biochem; 1983; 22: 4756-4763.

41. Kiski, G; Streaty, RA; and Klee, WA. Modulation of sodium-sensitive GTPase by partial opiate agonists. J Biol Chem; 1982; 257: 14035-14040.

42. Kloprogge, Ed; Akkerman, Jan Willem N. Binding kinetics of PAF-acether (1-O-alkyl-2-acetyl-*sn*-glycero-3-phosphocholine) in intact human platelets. J Biochem; 1984; 223: 901-909.

43. Kramp, R.M.; Pieroni, G.; Pinckard, R.N.; and Hanahan, D.J. Observations on the critical micellar concentrations of 1-O-alkyl-2-acetyl-*sn*-glyceryl-3-phosphorylcholine (PAF) and a series of its homologs and analogs. Chem Phys Lipids; 1984; 35: 49-62.

44. Laduron, Pierre M. Criteria for receptor sites in binding studies. Biochem Pharmacol; 1984; 33(6): 833-839.

45. Lee, TC; Malone, B; Wasserman, SI; Fitzgerald, V; and Snyder, F. Activities of enzymes that metabolize platelet activating factor (1-O-alkyl-2-acetyl-*sn*-glycero-3-phosphocholine) in neutrophils and eosinophils from humans and the effect of a calcium ionophore. Biochem Biophys Res Commun; 1982; 105: 1303-1308.

46. Lefort, J; Rotilio, D; and Vargaftig, BB. The platelet-independent release of thromboxane A_2 by PAF-acether from guinea pig lungs involves mechanisms distinct from those for leukotriene. Br J Pharmacol; 1984; 82: 565-575.

47. Maridonneau-Parini, I; Lagente, V; Lefort, J; Randon, J; Russo-Marie, F; and Vargaftig, BB. Desensitization to PAF-induced bronchoconstriction and to activation of alveolar macrophages by repeated inhalations of PAF in the guinea pig. Biochem Biophys Res Commun; 1985; 131: 42-49.

48. Marquis, O; Robaut, C; Cavero, I. [^{3}H]52770RP, a platelet-activating factor receptor antagonist, and tritiated platelet-activating factor label a common specific binding site in human polymorphonuclear leukocytes. J Pharm Exp Ther; 1988; 244(2): 709-715.

49. McManus, L.M.; and Pinckard, R.N. Kinetics of acetyl glyceryl ether phosphorylcholine (AGEPC)-induced acute lung injury in the rabbit. Am J Pathol; 1985; 121: 55-68.

50. McManus, L.M.; Hanahan, D.J.; Demopoulos, C.A.; and Pinckard, R.N. Pathobiology of the intravenous infusion of acetyl ether phosphorylcholine (AGEPC), a synthetic platelet activating factor (PAF), in the rabbit. J Immunol; 1980; 124: 2919-2924.

51. Mossmann, H.; Bamberger, U.; Velev, B.A.; Gehrung, M.; and Hammer, D.K. Effect of platelet-activating factor on human polymorphonuclear leukocyte enhancement of chemiluminescence and antibody-dependent cellular cytotoxicity. J Leuko Biol; 1986; 39: 153-165.

52. Motulsky, HJ; and Insel, PA. Influence of sodium on the $alpha_2$-adrenergic receptor system of human platelets. J Biol Chem; 1983; 258: 3913-3919.

53. Mueller, H.W.; O'Flaherty, J.T.; Greene, D.G.; Samuel, M.P.; and Wykle, R.L. 1-O-alkyl-linked glycerophospholipids of human neutrophils: Distribution of arachidonate and other acyl residues in the ether-linked and diacyl species. J Lipid Res; 1984; 25: 383-388.

54. Naccache, PH; Molski, MM; Volpi, M; Becker, EL; and Sha'afi, RI. Unique inhibitory profile of platelet activating factor induced calcium mobilization, polyphosphoinositide turnover and granule enzyme secretion in rabbit neutrophils towards pertussis toxin and phorbol ester. Biochem Biophys Res Commun; 1985; 130: 677-684.

55. Nadel, Jay A.; and Holtzman, Michael J. Regulation of airway responsiveness and secretion: role of inflammation. Asthma: Physiology, Immunopharmacology, and Treatment; 1984; III International Symposium: 129-155.

56. Ng, DS; and Wong, K. Platelet-activating factor stimulates phosphatidylinositol hydrolysis in human peripheral blood mononuclear leukocytes. Res Commun Chem Pathol Pharmacol; 1989; 66: 219-231.

57. O'Donnell, SR; Erjefalt, I; and Persson, CGA. Early and late tracheobronchial plasma exudation by platelet-activating factor administered to the airway mucosal surface in guinea pigs: effects of WEB 2086 and enprofylline. J Pharmacol Exp Ther; 1990; 254: 65-70.

58. O'Flaherty, J.T.; Surles, Jefferson R.; Redman, Jimmy; Jacobson, D; Piantadosi, C; Wykle, R L. Binding and metabolism of Platelet-activating factor by human neutrophils. J Clin Invest; 1986; 78: 381-388.

59. O'Flaherty, J.T.; Wykle, R.L.; Miller, C.H.; Lewis, J.C.; Waite, M.; Bass, D.A.; McCall, C.E.; and DeChatelet, L.R. 1-O-alkyl-*sn*-glyceryl-3-phosphorylcholines. A novel class of neutrophil stimulants. Am J Pathol; 1981; 103: 70-78.

60. Oda, M.; Satouchi, K.; Yasunaga, K.; and Saito, K. Molecular species of platelet-activating factor generated by human neutrophils challenged with ionophore A23187. J Immunol; 1985; 134: 1090-1093.

61. Page, CP; Guerreiro, D; Sanjar, S; and Morley, J. Platelet activating factor (PAF-acether) may account for late-onset reactions to allergen inhalation. Agents Actions; 1985; 16: 30-32.

62. Pfeiffer, A; Sadee, W; and Herz, A. Differential regulation of the mu-, delta-, and kappa-opiate receptor subtypes by guanyl nucleotides and metal ions. J Neurosci.; 1982; 2,7: 912-917.

63. Pinckard, R.N.; Jackson, E.M.; Hoppens, C.; Weintraub, S.T.; Ludwig, J.C.; McManus, L.M.; and Mott, G.E. Molecular heterogeneity of platelet-activating factor produced by stimulated human polymorphonuclear leukocytes. Biochem Biophys Res Commun; 1984; 122: 325-332.

64. Pinckard, RN; Ludwig, JC; and McManus, LM. Platelet activating factors. New York: Raven Press, Ltd; 1988.

65. Pong, S-S; and DeHaven, RN. Characterization of a leukotriene D4 receptor in guinea pig lung. Proc Natl Acad Sci USA; 1983; 80: 7415-7419.

66. Ponpipom, MM; Hwang, S-B; Doebber, TW; Acton, J; Alberts, AW; Biftu, T; Brooker, DR; Bugianesi, RL; Lam, M-H; and Wu MS. (+)-trans-2-(3-methoxy-5-methylsulfonyl-4-propoxyphenyl)-5-(3,4,5-trimethoxyphenyl) tetrahydrofuran (L-659,989), a novel, potent PAF receptor antagonist. Biochem Biophys Res Commun; 1988.

67. Pretolani, M; Lefort, J; Malanchere, E; Vargaftig, BB. Interference by the novel PAF-acether antagonist WEB 2086 with the bronchopulmonary responses to PAF-acether and to active and passive anaphylactic shock in guinea pigs. Eur J Pharmacol; 1987; 140: 311-321.

68. Ramesha, C.S.; and Pickett, W.C. Species-specific variations in the molecular heterogeneity of the platelet-activating factor. J Immunol; 1987; 138: 1559-1563.

69. Reed, C.E. New Therapeutic Approaches in Asthma. J Allergy and Clin Immunol; 1986; 77(4): 537-543.

70. Robaut, C; Durand, G; James, C; Lave, D; Sedivy, P; Floch, A; Mondot, P; Pacot, D; Cavero, I; Furle, G. PAF Binding Sites. Characterization by [3H]52770 RP, a pyrrolo [1,2-c]thiazole derivative, in rabbit platelets. Biochem Pharmacol; 1987; 36(19): 3221-3229.

71. Roberts, NM; McCusker, M; Chung, KF; and Barnes, PJ. Effect of a PAF antagonist, BN52063, on PAF-induced bronchoconstriction in normal subjects. Br J Clin Pharmacol; 1988; 26: 65-72.

72. Rodbard, D; and Frazier, GR. Statistical analysis of radioligand assay data. Methods Enzymol; 1975; 37: 3-22.

73. Rosenthal, H. Graphic method for the determination and presentation of binding parameters in a complex system. Anal Biochem; 1967; 20: 525-532.

74. Scatchard, G. The attraction of proteins for small molecules and ions. Ann NY Acad Sci; 1949; 51: 660-672.

75. Schoenbechler, M.J.; and Barbaro, J.F. The requirement for sensitized lymphocytes in one form of antigen-induced histamine release from rabbit platelets. Proc Natl Acad Sci U S A; 1968; 60: 1247-1251.

76. Shaw, JO; Pinckard, RN; Ferrigni, KS; McManus, LM; and Hanahan, DJ. Activation of human neutrophils with 1-O-hexadecyl/octadecyl-2-acetyl-*sn*-glyceryl-3-phosphorylcholine (platelet-actiavting factor). J Immunol; 1981; 127: 1250-1255.

77. Siraganian, RP.; Osler, AG. Antigenic release of histamine from rabbit leukocytes. Immunol; 1970; 104(6): 1340-1347.

78. Stenton, SC; Court, EN; Kingston, WP; Goadby, P; Kelly, CA; Duddridge, M; Ward, C; Hendrick, DJ; and Walters, EH. Platelet activating factor in bronchoalveolar lavage fluid from asthmatic subjects. Eur Respir J; 1990; 3: 408-413.

79. Stimler, N. P.; O'Flaherty, J. T. Spasmogenic properties of platelet-activating factor: Evidence for a direct mechanism in the contractile response of pulmonary tissues. Am J Pathol; 1983; 113: 75-84.

80. Stimler, NP; Gerard, C; and O'Flaherty, JT. Contraction of human lung tissues by platelet-activating factor (AGPC). INSERM; 1983; 23: 195-204.

81. Terashita, Z-I; Imura, Y; Nishikawa, K. Inhibition by CV3988 of the binding of [3H]-Platelet Activating Factor (PAF) to the platelet. Biochem Pharmaco; 1985; 34(9): 1491-1495.

82. Ukena, D; Dent, G; Birke, FW.; Robaut, Ch; Sybrecht, GW.; Barnes, PJ. Radioligand binding of antagonists of platelet-activating factor to intact human platelets. FEBS Letters; 1988; 228(2): 285-289.

83. Valone, F.H.; Coles, E.; Reinhold, V.R.; and Goetzl, E.J. Specific binding of phospholipid platelet-activating factor by human platelets. J Immunol; 1982; 129: 1637-1641.

84. Valone, FH. Identification of platelet-activating factor receptors in P388D1 murine macrophages. J Immunol; 1988; 140(7): 2389-2394.

85. Wardlow, ML; Cox, CP; Meng, KE; Greene, DE; and Farr, RS. Substrate specificity and partial characterization of the PAF-acylhydrolase in human serum that rapidly inactivates platelet-activating factor. J Immunol; 1986; 136: 3441-3446.

86. Wasserman, SL. Platelet-activating factor as a mediator of bronchial asthma. Hosp Pract; 1988: 49-58.

87. Weiland, Gregory A.; Molinoff, Perry B. Quantitative analysis of drug-receptor interactions: I. Determination of kinetic and equilibrium properties. Life Sciences; 1981; 29: 313-330.